Optimization of Drilling Fluid Flow Rates – A Study of the Drilling Fluid Flow rates and Annular Pressure in Horizontal Directional Drilling

by

Bingxuan Li

A thesis submitted in partial fulfillment of the requirements for the degree of

Master of Science

in

Civil (Cross-disciplinary)

Department of Civil and Environmental Engineering

University of Alberta

© Bingxuan Li, 2023

Abstract

Trenchless technologies have experienced the fast development and dramatic change in the past three decades. Derived from oil and gas industry, Horizontal Directional Drilling (HDD) is considered as one of the most rapidly expanded trenchless technologies and widely used in infrastructure construction and pipeline installation, minimizing the social, environmental, and economic cost compared with traditional open cut method.

In the HDD, drilling fluid plays an important role in borehole integrity and cuttings transportation. However, improper drilling fluid management is directly related to several frequent problems in drilling process, including insufficient hole cleaning performance and hydro fracture. Excess drilling fluid flow rate will increase the borehole annular pressure, and further raise the risk of hydro fracture in the annulus, while low drilling fluid flow rate will affect the hole cleaning performance and lead to stuck pipe. Due to the HDD unique features such as large borehole diameter, highly inclined and horizontal borehole, previous models for drilling fluid management developed in oil and gas industry perform poorly in HDD project.

To have a brief understanding of drilling fluid flow rate limitation, a comprehensive review was conducted. Annular pressure and hole cleaning performance were found to be the most important factors which restricted the drilling fluid flow rate. The Delft equation, which was considered as the widely accepted solution to estimate the maximum allowable

pressure in the borehole, was analyzed to calculate the maximum flow rate along the drill path. Five different cuttings transport models were introduced and compared to quantify the minimum drilling fluid flow rate in the annulus.

Among the five different models, Larsen's model was employed to a case study to verify its feasibility and accuracy in HDD industry. Although Larsen's model had some defects, it provided a reference value (critical transport fluid velocity) indicating when the cuttings stopped accumulating in the lower side of wellbore and roughly estimated the cuttings bed heigh when drilling fluid flow rate was relatively low. Overall, Larsen's model had a high potential to become an indicator for hole cleaning performance

Another case study was conducted to analyze the maximum flow rate change with the Delft Equation. The maximum flow rate raised to a peak point and decreased in the remaining drilling path. The peak point occurred when the increment of the maximum frictional pressure loss equaled to the frictional pressure loss gradient. The annular pressure easily exceeded the maximum allowable pressure near the entry and exit point, which meant that adequate reinforcement and casing were necessary in the exit and entry point. Most of the drill path (80%), drilling fluid could be circulated at 0.5 m/s and over half of the drill path (55%) drilling fluid could be circulated at 5 m/s. As a result, drilling fluid could be circulated at a dynamic flow rate in different sections of drill path, which would greatly improve the hole cleaning performance in the annulus.

Preface

This thesis is an original work by Bingxuan Li, and paper based.

Acknowledgements

I would like to express my deepest application to my supervisor, **Dr. Alireza Bayat**, for his continuous guide, support, and encouragement throughout my graduate study in the past years. His valuable comments, ideas and dedication inspire me to think critically and solve academical problems in the past two years.

I also appreciate the time and help from Dr. Ergun Kuru, for his ideas and guide for my topic.

I would also like to express my gratitude to Dr. Chao Kang and Dr. Sheng Huang, for their instructions at the beginning of my graduate study, and Dr. Shadi Ansari for her edition comments for my graduate thesis.

I would like to thank our research coordinator Lana Gutwin, for her contributions in research and experiment arrangement.

My sincere thanks to my MSc thesis defense committee members, for their valuable time and help.

Finally, I would like to express my appreciation to my family for their continuous love and support in my life.

Table of Contents

List of Tables

List of Figures

Chapter 1: Introduction

1.1 Background

Trenchless construction is defined as a series of methods, materials, and equipment used for the installation, replacement or rehabilitation of existing underground infrastructure with minimal disruption to surface traffic, business, and other activities (Zaneldin, 2006; Ariaratnam et al., 1999). The application of trenchless technology is applicable for wide range of applications in situations as wide-ranging from tunnels for sewers or water pipelines a few meters in diameter, to the smallest pipes and cables-typically one or two centimeters only (Thomson and Rumsey, 1997). New trenchless construction techniques include horizontal directional drilling (HDD), micro tunneling (MT), pipe jacking (PJ), auger boring (AB), and pipe bursting (PB) (Ariaratnam et al., 1999). Trenchless rehabilitation techniques include the lining of pipe (LP), pipe scanning and evaluation (PS&E), and robotic spot repair (RSR) (Ariaratnam et al., 1999). Trenchless technologies that are expected to experience the greatest future growth are auger boring, pipe jacking, and horizontal directional drilling for the growing demand for new construction and lining of pipes for rehabilitation (Zaneldin, 2006).

Horizontal Directional Drilling (HDD), with origins in the oil and gas industry, is a trenchless technology employed to install underground pipelines with minimal impacts on

the environment or damage to existing infrastructure such as roadways and other surface structures (Yan et al. 2018). HDD is a relatively new construction technology that combines the directional drilling technology in petroleum engineering with the traditional pipeline construction method. In comparison with other trenchless technologies, HDD offers several advantages: (1) No vertical shafts are required as drilling commences from the surface; (2) relatively short setup time; (3) the borehole alignment does not necessarily have to be straight, and (4) higher installation length compared with any other non-man entry trenchless method (Allouche and Ariaratnam 2000). HDD make it possible to change the borehole alignment and elevation to avoid striking existing utilities and other underground obstacles along the path (Allouche and Ariaratnam 2000).

It might be said that HDD has outgrown its infancy stage but is yet to achieve the status of a mature industry (Allouche and Ariaratnam 2000). As the HDD was developed from well drilling in petroleum engineering, it also has similar technical problems in vertical well drilling, such as insufficient hole cleaning performance and excessive annular pressure. Compared with directional drilling in Petroleum Engineering, HDD has a shallower cover depth and larger borehole diameter, which makes some problems more serious, such as hydro fracture, pipe blocking, etc. Generally, the borehole becomes less stable with decreasing cover depth (Deng, 2018). The large borehole diameter makes it hard to accomplish turbulent flow in the annulus, which is not ideal for cuttings removal. In the drilling process, drilling fluid plays an important role. Drilling fluid is comprised of

carrying medium (water or oils), bentonite and various additives, which is considered as a major factor in the cost and success of geothermal drilling operations (Mohamed et al. 2021; Chemwotei, 2011; Vivas et al., 2020). In HDD projects, water-based drilling fluid is widely used during pilot boring, reaming, and pullback processes. The functions of drilling fluids include carrying drilled cuttings and transporting them to the surface; suspending the drilled cuttings when the circulation is stopped; cooling and cleaning the bit; maintaining the stability of the wellbore, etc. (Menezes et al. 2010; Caenn et al., 2011; Caenn and Chillingar, 1996; Luckham and Rossi, 1999)

The key to improve the drilling efficiency and hole cleaning performance is to control the drilling fluid in the annulus. To ameliorate the drilling fluid performance, one option is to adjust different drilling fluid rheological properties by changing the compositions of drilling fluid. Rheology is defined as the science and study of the deformation and flow of matter, including its elasticity, plasticity, and viscosity (Baumert ta al., 2005). Drilling fluid is comprised of water, bentonite and multiple additives. Additives such as Xanthan gum, hydroxyethyl cellulose (HEC), partially hydrolyzed polyacrylamide (PHPA), nano-silica, carboxymethyl cellulose (CMC), low-viscosity and regular polyanionic cellulose (PAC-L and PAC-R) are added to drilling fluid to change the drilling fluid rheological properties for different purposes. For example, the applicable concentration of HEC in drilling fluid gives a sufficient viscosity to transport and suspend cuttings (Ouaer and Gareche, 2018).

Another solution for improving drilling fluid performance is to increase the flow rate of

drilling fluid in the annulus. Raising the annular drilling fluid rate is considered as a convenient and efficient way to improve the cuttings removal process in the annulus and drilling performance in the drilling bit. In the lower side of annulus, removed cuttings may settle down and form stational bed. Cuttings bed erosion occurs at a faster rate as the drilling fluid flow rate increases (Adari et al. 2000). However, the drilling fluid flow rate could not be increased without limitation. High flow rate increases the risk of hydro fracture and drilling fluid leakage, which is not preferred for hole stability. Low flow rate may not be able to transport cuttings to surface, which will cause blocking of the drilling pipe or product pipe.

As a result, how to dynamically quantify the upper limitation of flow rate during HDD to maintain drilling fluid flow rate as large as possible comes to our view. To control drilling fluid flow rate properly could enhance cuttings transport performance and avoid unnecessary risks such as hydro fracture and pipe blocking. This thesis will focus on management of drilling fluid flow rate in the pilot boring stage, which have high risk of hydraulic fracture.

1.2 Research Objectives

The main research objectives are to

Objective 1: Discuss the mechanism of cuttings transport and analyze various models designed for minimum drilling fluid flow velocity.

Objective 2: Verify the feasibility of Larsen's model in HDD pilot boring stage with a case study done by Xiang's (2016) project.

Objective 3: Quantify annular pressure and the maximum allowable pressure in the borehole.

Objective 4: Define upper boundary of drilling fluid flow rate with their variation during the drilling process and design a better-performed flow rates distribution.

1.3 Methodology

A comprehensive review of possible influential factors which restrict the drilling fluid flow rates in the annulus were discussed in the literature review parts, to identify the limitation of flow rates. After classification of all parameters, various calculations were conducted to estimate the upper boundary and lower boundary of the flow rates as well as their trends varied with the drilling process. Five different empirical and theorical approaches were compared and evaluated. A case study provided by Xiang (2016) was picked to validate the accuracy of Larsen's model in calculating the drilling fluid minimum flow rate and

predicting the cuttings concentration. In the case study, four kinds of drilling fluid with different drilling fluid rheological properties were used. The critical transport velocity (CTFV), cuttings concentration and corresponding cuttings bed heights were calculated and compared with the measured values. The accuracy and feasibility of Larsen's model in HDD was investigated.

Another case study designed to analyze the maximum flow rate change throughout the drilling process based on the Delft Equation. The trend of maximum flow velocity along the drill path was plotted and discussed. The peak value of the maximum velocity was calculated and evaluated. Maximum flow velocity distribution and a suggested segmented flow velocity design was analyzed and summarized. Recommendations will be concluded based on the case study results.

1.4 Outline of Thesis

This thesis describes the following structure:

Chapter 1: Introduction

The chapter covered a brief introduction to trenchless technology and Horizontal Directional Drilling (HDD), with the objectives and methodology of the thesis

Chapter 2: Literature Review

The chapter introduced various up-to-date studies regarding to the cuttings transport

mechanisms and models, minimum flow velocity, Delft Equation, and maximum flow rate

Chapter 3: Feasibility of Larsen's model for minimum drilling fluid velocity in HDD pilot boring stage

The chapter applied a case study about the horizontal wellbore with all necessary data to Larsen's model to obtain the critical transport fluid velocity (CTFV) and cuttings concentration. The feasibility and accuracy of Larsen's model in predicting the cuttings concentration in small scale horizontal annulus were compared and discussed.

Chapter 4: Application of Delft Equation to estimate the maximum drilling fluid flow rate in HDD

The chapter researched the maximum allowable pressure throughout the bore path and obtained a variation curve. Drilling fluid hydrostatic pressure and maximum frictional pressure loss were also calculated. The variation curves of the maximum flow rates along the borehole were discussed. The maximum flow velocity distribution and a suggested segmented flow velocity design were displayed.

Chapter 5: Conclusion and future research

This chapter listed the key conclusions of the thesis with the recommendations on future research.

Chapter 2: Literature Review

2.1 Introduction

Trenchless technology is arguably the fastest-expanding technology affecting the world's construction industry today (Jung and Sinha, 2007). It can be defined as a group of methods for constructing and rehabilitating underground utilities that require minimal surface excavation and provide important new alternatives to traditional open-cut methods of utility pipe installation (Suleiman et al., 2010). Table 2.1 introduces a series of trenchless technologies.

Table 2.1. Trenchless Technologies used in industry (Suleiman et al., 2010; Najafi, 2005)

Method	Diameter Range (in)	Maximum installation (ft)	Applications	Installation Accuracy
Pipe jacking and conventional tunneling	>= 42	1500	Pressure and gravity pipe	± 1 in
Auger boring	4 ~ 60	600	Road and rail crossing	± 1% of the bore length
Microtunneling	10 ~ 136	500-1500	Gravity pipe	± 1 in
Mini-HDD	2 ~ 12	600	Pressure pipe/cable	Varies
Midi-HDD	12 ~ 24	1000	Pressure pipe	Varies
Maxi-HDD	24 ~ 48	6000	Pressure pipe	Varies
Pipe ramming	< 120	400	Road and rail crossing	Dependent on setup
Compaction methods	< 8	250	Pipe or cable	± 1 in

Among various trenchless technologies, Horizontal directional drilling (HDD) technology

enables the installation of conduits and pipelines ranging from 50 mm (2 in.) to 1,200 mm (48 in.) in diameter over extensive distances, up to 1,800 m (6,000 ft), with minimum need for open-cut surface excavation (Ariaratnam et al., 2004). HDD could be classified as Mini-HDD, Midi-HDD and Maxi-HDD based on the design diameter and maximum installation length. HDD was used for the first time by the Pacific Gas and Electric Co. for crossing Pajaro River near Watsonville, California in 1971 to install the 4-inch in diameter of steel pipe for a drive length of 615 ft (Sarireh et al. 2012). Today, with the development of HDD innovations, it has become an important and effective method for pipeline installation in different uses including product oil, natural gas, water, sewer, electrical and telecommunications (Ma and Najafi, 2008; Yan et al. 2018).

HDD consists of three main steps in the construction process: 1) drilling of the pilot hole, 2) reaming of the pilot hole, and 3) pulling back of pipe string (Balcay and Baser 2019).

Stage 1: Pilot boring

The first stage is to drill pilot hole along the designed path with drilling bit. Entry point with exit point need to be designed before drilling and proper bit should be chosen based on soil conditions. Guiding technologies such as cable locator and Ground-penetrating Radar (GPR), are used to detect the obstacles and direct the drilling. Among three stage, pilot boring has the greatest construction concern due to the high risk of hydraulic fracture and loss of drilling fluid circulation (Rostami, 2017). Figure 2.1 shows the pilot boring

process.

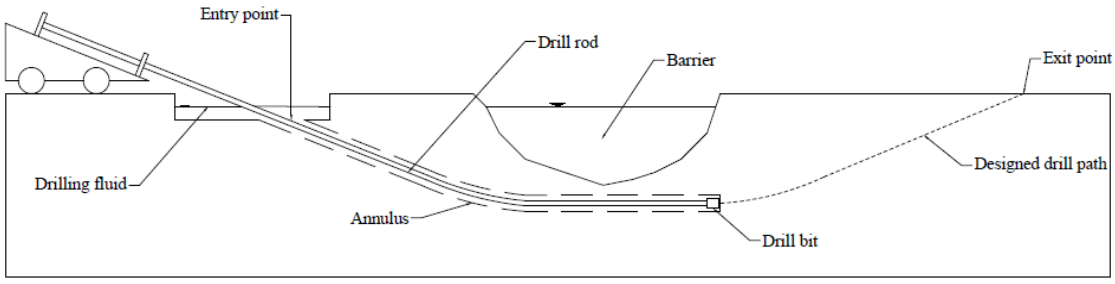

Figure 2.1. Pilot boring from entry point (Moganti 2016; J. D. Hair & Associates Inc., 2010)

For long river crossings or Maxi-HDD operations, some projects may choose to drill 2 pilot holes from the entrance and exit point at the same time. Rotary magnet orientation intersects (RMOI) technology will be used for guiding the drilling process to make 2 pilot holes meet in the designed point (Yan et al. 2018). Figure 2.2 shows the pilot boring from 2 directions.

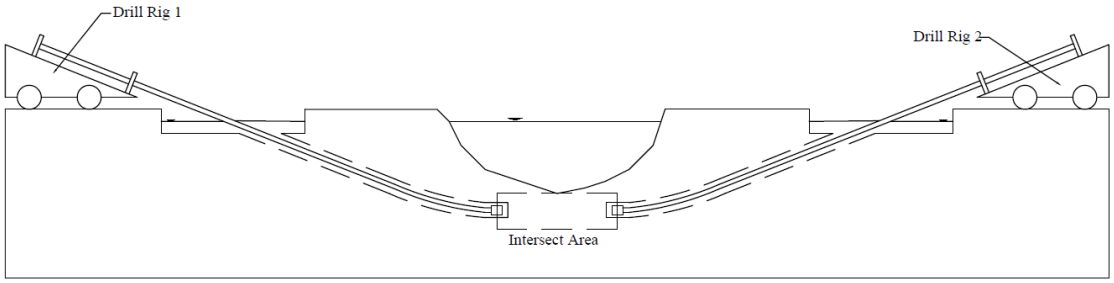

Figure 2.2. Pilot Holes from 2 directions (Yan et al. 2018)

Stage 2: Reaming

The second stage of the HDD project is reaming. Reamers will be pulled through the previous pilot hole to enlarge the borehole diameter, accommodating for the installation of pipes. The size and type of the reamer depend on the size of the product pipe and geological conditions (Moganti 2016). The reaming process may be repeated multiple times, which depends on the diameter of the pipe, soil characteristics and reamer performance. Figure 2.3 shows the reaming process.

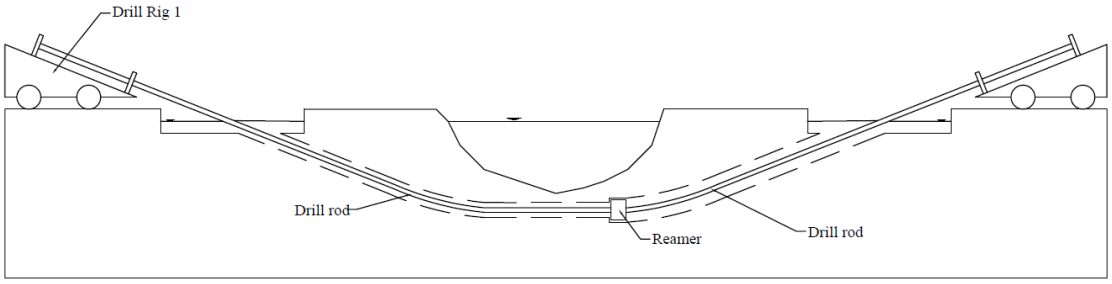

Figure 2.3 Reaming process (Moganti 2016; J. D. Hair & Associates Inc., 2010)

Stage 3: Pull back

The final stage is to pull the pipe in. This process is usually combined with the last reaming process. During this stage, the drilling fluid is still circulated in the annulus to help lubricate the product pipe. Figure 2.4 shows the pullback process.

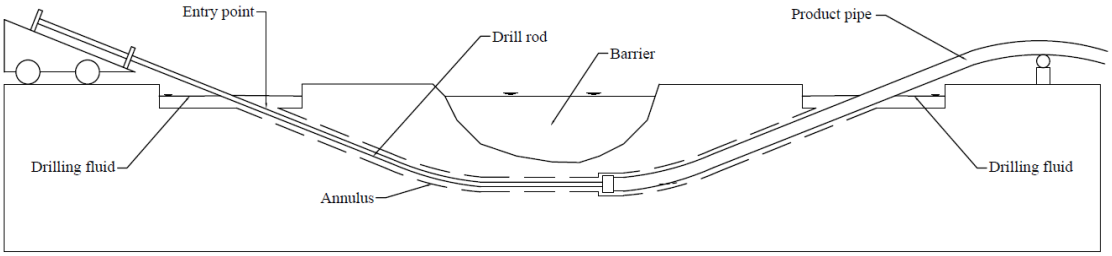

Figure 2.4. Pullback process (Moganti 2016; J. D. Hair & Associates Inc., 2010)

In HDD construction, drilling fluid plays an important role in the whole process. Many serious problems are directly caused by improper management of drilling fluid, such as blocking of the drilling pipe or product pipe, hydraulic fracturing, drilling fluid seepage, etc. Increasing the drilling fluid flow rate could remarkably increase the hole cleaning performance by removing the cuttings from the borehole. But very high flow rates are not preferred to borehole stability, due to the increase of annular pressure. As a result, controlling the drilling fluid rates is a vital requirement to prevent borehole failures. To balance the flow rate in the annulus between maintaining borehole integrity and sufficient hole cleaning performance remains a remarkable topic.

This chapter provides reviews of previous research about drilling fluids, drilling fluid flow rate as well as possible borehole failure related to drilling fluids and limitations of drilling fluid flow rate in the annulus. The mechanism of cuttings transport is explained, and different models designed to estimate minimum flow velocity are detailly introduced and compared. Maximum borehole pressure with upper boundary of flow rate is discussed. Delft Equation and some other theories are illustrated. Borehole path design is also mentioned in this chapter.

2.2 Borehole path design

An optimal drill path design requires consideration to constraints resulting from the surface

topography, obstacles, allowable drill pipe and product pipe bending stresses, the geological profile, geotechnical parameters and drilling fluid pressures (Murray et al., 2014). Approximate locations for the entry and exit points of the drilling path are decided after completing a preliminary study that also assesses the relevance of HDD for the project at stake (Patino-Ramirez et al., 2020).

The geometric alignment consists of at least 5 segments, starting with an entry tangent from the rig side, followed by a curved segment that reaches the central portion of the alignment (Patino-Ramirez et al., 2020). The remaining segments are horizontal tangent, exit radius and exit tangent. 5-segment drill path is usually suitable for most of HDD project A brief Figure 2.5 is showed below to illustrate the drill path (Murray et al., 2014).

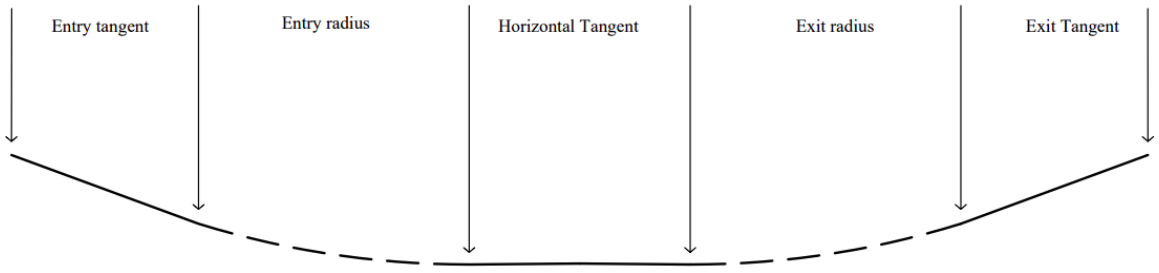

Figure 2.5 Brief description of HDD drill path design (Murray et al., 2014)

Borehole entrance angle is usually set between 8 degree and 16 degree (20 degree at most) from horizontal and exit angle varies from 5 degree to 10 degree from horizontal, which means that the slope in the whole drilling will be smaller than 20 degrees. Among this range, cuttings bed was formed but did not slide downward even when drilling fluid

circulation was stopped (Luo, 1988). Accumulation of cuttings bed in HDD led to different minimum transport velocity compared with vertical well, which became the major concern in the cutting transport. The annular pressure and maximum allowable pressure vary during the drilling process with the changing depth and borehole length, showing different trends in different segments. The change in annular pressure, maximum allowable pressure and cuttings slip velocity will be discussed in detail in the thesis.

2.3 Drilling Fluid

The drilling fluid in the drilling process can be seen as the equivalent to the blood in the human body, the mud pump is the heart, and the drilled-out shale (cuttings) represent the slag products (Skalle, 2013). In Horizontal Directional Drilling, drilling fluid is composed of a carrier fluid (water) and drilling fluid additives (bentonite and/or polymers) (Ariaratnam et al., 2004). The fundamental use of the drilling fluid is to establish and maintain the bore hole integrity, including chemical stability and mechanical stability, by the formation of the mud cake and remove cuttings from the drilling bit and annulus. Other principal functions of the drilling fluid includes (1) cooling and cleaning the bit; (2) reducing friction between the drilling string and the side of the hole; (3) preventing inflow of fluids from permeable rocks penetrated; (4) forming a thin, low-permeability filter cake which seals pores and other openings in formation penetrated by the bit, and (5) assistant in the collection and interpretation of information available from drilling cuttings, cores, and electrical logs (Apaleke et al., 2012;Hossain and Al-Majeed, 2012).

To optimize the drilling fluid performances, some fundamental parameters are considered first, such as fluid density, viscosity, and fluid loss (Khodja et al., 2010). Proper drilling fluid density is designed to balance the pore pressure and annular pressure, which should be adjusted to ground conditions. Mud must be viscous enough in order to be able to lift the cuttings to the surface, but at the same time, viscosity must not be too high in order to minimize friction pressure loss (Khodja et al., 2010). A number of factors affect the fluid-loss properties of a drilling fluid, including time, temperature, cake compressibility; but also, the nature, amount and size of solids present in the drilling fluid (Khodja et al., 2010).

These changes are mainly achieved by changing the composition of drilling fluid and adding different additives. Approximately 5000 different additives (Skalle, 2013) are used to modify the drilling fluid rheological properties for different purposes. Clays, polymers, weighting agents, fluidloss-control additives, dispersants or thinners, inorganic chemicals, lost-circulation materials, and surfactants are the most common types of additives used in water-based muds (Mitchell and Miska, 2011).

Changing the drilling fluid rheological properties is an effective way to improve the drilling fluid performances, especially hole cleaning performance. Different additives provide different functions to the drilling fluids, like modifying rheology, reducing filtration loss, enhancing lubrication, prohibiting clay swelling etc. (Deng, 2018)

However, another common and convenient practice is to increase the drilling fluid flow

rate in the annulus. Increasing the drilling fluid flow rate will greatly reduce the volumetric fraction of cuttings in the circulating drilling fluid (Hussaini and Azar 1983; Tomren et al. 1986). Ideally, the volumetric fraction of solids should be maintained as low as possible in order to achieve the highest possible hole cleaning performance during HDD operations (Su, 2020). In practice, a proper volumetric fraction of cuttings will be chosen based on ground conditions and economic considerations. At higher solid volumetric fractions, the drastically increasing friction pressure loss will significantly increase the risks associated with hydro fracturing (Su, 2020).

Fluid flow velocity is the dominant drilling variable in hole cleaning due to its direct relation with the shear stress acting on the cuttings bed (Ozbayoglu et al., 2010; Kjosnes et al., 2003). High flow velocity has a positive contribution to removal of stationary bed, which is more significant in higher hole inclinations and higher fluid viscosities (Piroozian et al., 2012). The cuttings bed erosion affected by the drilling fluid flow is also dependent on the cuttings bed properties. If the cuttings bed is loose and porous, it is only necessary to remove single cuttings particles that are not adhered to the bed (Saasen and Løklingholm, 2002). In this case, high flow velocity is sufficient to remove the cuttings from the cutting bed. In the opposite case, if the cuttings bed is well consolidated and no cuttings particles are free to be removed alone from the bed by the flow, hole-cleaning is difficult (Saasen and Løklingholm, 2002). Once cuttings settle down and form a cuttings bed in the invent of borehole, it is hard to clean up the borehole by increasing Yield Point of mud or pump

volume in both of directional and inclined HDD borehole (Zeng et al., 2018). So, the drilling pipe rotation is very important in hole cleaning performance, while the drill pipe drags a large portion of the bed around from the bottom of the annulus to the top where the high flow rate is (Saasen and Løklingholm, 2002).

However, although high drilling fluid flow rate could improve the drilling fluid performance, it also increases the frictional pressure loss in the annulus, which raise the risk of hydro fracture in the annulus. Low flow rate will affect the hole cleaning performance, which may lead to stuck pipe, and also increase the risk of hydro fracture due to the high volumetric fraction of cuttings. In this case, the limitations for drilling fluid flow rates need to be quantified and an adequate flow rate should be designed carefully. High drilling fluid flow rates are required to be restricted to keep the borehole stable and minimum flow rate should be guaranteed to remove cuttings from the annulus.

2.4 Drilling Fluid Flow Regime

The drilling fluid flow regime in the annulus could be classified into 3 categories, laminar flow, turbulent flow and laminar – turbulent transition. In a laminar flow, the fluid behaves like a series of parallel layers moving at uniform or near-uniform velocity, where no large-scale movement of fluid particles between layers (Guo and Liu, 2011). On the other hand, turbulent flow is chaotic in nature and very irregular in both time and space; for example, velocity in a turbulent flow is a function of space and time which makes the modeling and

prediction of behavior of a turbulent flow through theoretical analysis impossible (Bizhani, 2013).The laminar–turbulent transition in the boundary layer is a continuous process beginning from the instant of disturbance generation and ending at the instant of final establishment of a developed turbulent flow (Boiko et al., 2015).

Reynolds number is commonly calculated to determine the flow regime. Laminar usually occurs with Reynolds number which is approximately smaller than 2000 and turbulent flow forms with Reynolds number which is larger than 4000. When Reynolds number is between 2000 and 4000, the flow is usually considered as laminar–turbulent transition.

In general, both laminar and turbulent flow can be used effectively for hole cleaning in vertical flow (Tomren et al., 1986). However, Tomren et al. (1986) found that cuttings-transport performance in inclined wells and horizontal wells will be worse in laminar flow than in turbulent flow, provided that both fluids have adequate effective viscosity (Tomren et al., 1986). Cuttings removal was easier with turbulent flow than with laminar flow (Adari et al. 2000). Luo (1988) considered improvement of cuttings transport under turbulent flow may be attributed to (1) the flattened fluid velocity profile, thus higher fluid velocity in the near-wall region and smaller "torque effect"; (2) the destructive action of the countless eddies and swirls in turbulent flow on the cuttings bed in inclined annuli (Luo, 1988).

In HDD the large annular space and limited pump pressure, as well as the high risk of hydro fracture all, imply that pumping drilling fluids, even water, in turbulent flow is impractical

(Deng, 2018; Shu et al. 2015). The flow regime in the annulus is usually considered as laminar flow in HDD project.

2.5 Limitation for drilling fluid flow rate

Although high drilling fluid flow rate could improve the drilling fluid performance, it also increases the frictional pressure loss in the annulus, which raise the risk of hydro fracture in the annulus. As a result, the annular pressure profile needs to be sufficient to support the borehole annulus and not exceed the maximum allowable pressure of the overburden (Murray et al., 2014). Low drilling fluid flow rate increases the risk of hydro fracture due to the high volumetric fraction of cuttings and goes against sufficient hole cleaning performance. The most common drilling problems related to insufficient hole cleaning occurs during tripping and reaming operation (Skalle, 2011).

In this case, the limitations for drilling fluid flow rates need to be quantified and an adequate flow rate should be designed carefully. High drilling fluid flow rates need to be restricted to keep the borehole stable and minimum flow rate should be guaranteed to remove cuttings from the annulus.

2.6 Minimum Flow rate (HDD industry estimation)

Of the many functions that are performed by the drilling fluid, the most important is to transport cuttings from the bit up the annulus to the surface (Mitchell and Miska, 2011). A

minimum drilling fluid flow rate is required for carrying drill cuttings to the surface (Boyun and Gefei, 2011). In the Horizontal Directional Drilling project, the drilling fluid flow rate are set based on cuttings production rate and soil conditions. On the other hand, Oil and gas engineering also considered the minimum mud velocity based on particle slip velocity.

The minimum flow rate in Horizontal Directional Drilling project is proportional to the cuttings production rate, which could be calculated as:

$$Q_{fluid} = C_s * Q_c \quad (2\text{-}1)$$

The symbols are defined below:

Q_{fluid}: Drilling fluid flow rate (m^3/min)

C_s : Fluid-to-soil ratio, depends on soil conditions

Q_c: Cutting's production rate (m^3/min)

The cutting's production rate is related to the cross-section area of the borehole, rate of penetration and soil conditions, which could be calculated from Mitchell and Miska's book (2011) with the formula 2-2:

$$Q_c = A_{hole} * ROP * (1 - porosity) \quad (2\text{-}2)$$

The symbols are defined below:

A_{hole}: Cross section area of the borehole (m^3).

ROP: Rate of Penetration (m/h).

$porosity:$ Porosity of the soil.

Different fluid-to-soil ratios are picked based on different soil conditions. For example, a value of 2 to 3 is usually chosen for sand. Su's (2020) thesis recommended that the volumetric fraction of sands should be maintained below 30-35% wherever possible, in order to prevent excessively high annular friction pressure loss and to minimize the risk of hydro fracture. Vermeer Corporation also posted a table of suggested value for fluid-to-soil ratios, which is shown in Table 2.2 (Vroom, 2018):

Table 2.2 Suggested drilling fluid/cuttings ratio for different soil types (Vroom, 2018)

Soil	Factor of Safety (Drilling Fluid/cuttings)
Sand, Gravel, Cobble	1:1 or 2:1
Fine sand, clay-like sand	2:1 or 3:1
Sandy clay	3:1 or 4:1
Reactive clay	5:1 or more

2.7 Minimum mud velocity

2.7.1 Introduction

Another important concept which limits the drilling fluid flow rate is the minimum drilling fluid velocity, also called minimum transport velocity (MTV) or critical fluid velocity (CFR). The underlying principle of the MTV concept is that solids in subsea tiebacks will be transported as long as they are upwardly mobile whether by rolling/sliding along the

low side wall of a pipeline or in heterogenous suspension (Bello et al., 2011). The MTV is in fact a measure of the drilling fluids' cuttings carrying capacity, in that the lower the MTV, the greater the carrying capacity of the fluid (Ford et al., 1990).

Ford et al. (1990) concluded 7 different transport patterns in the annulus, which are homogeneous suspension, heterogeneous suspension, saltation, sand clusters, separated moving beds, continuous moving bed and stationary bed. They also raised two different mechanisms used to describe the cuttings transport profile. The first is whereby the cuttings are transported up the annulus rolling or sliding along the low side wall and the second is where the cuttings are transported in suspension in the flowing annular fluid (Ford et al., 1990). MTV for suspension is the velocity above which the mixture flows in asymmetric suspension pattern or the velocity below which solids form a deposit on the bottom of the pipe (Bello and Oyeneyin, 2016). When drilling fluid is circulated at MTV for suspension, cuttings transport patterns tend to be homogeneous, heterogeneous, saltation or salt clusters. For velocity below the MTV for suspension will result in the solids sliding along the pipe wall which may eventually result in stationary bed as the pressure drops along the pipeline causing further reduction in the particle drag forces (Bello et al., 2011). MTV for rolling is the velocity at and above which a moving bed of particle exists on the bottom of the pipe and some particles moved by saltation or the velocity below which the part of the bed in contact with the pipe wall becomes stationary (Bello and Oyeneyin, 2016). Separated moving bed, continuous moving bed and stational bed are the common cuttings transport

patterns when drilling fluid is circulated in MTV for rolling. Table 2.3 (Ford et al., 1990) illustrates the features of 7 different flow patterns.

Table 2.3. Various flow patterns for cuttings suspension and rolling (Ford et al., 1990)

Transport type	Flow pattern	Description
Suspension	Homogeneous	Cuttings are transported in suspension and distributed uniformly in annulus.
	Heterogeneous	Cuttings concentration is different, where the cuttings concentration in lower side is higher than the upper side of the annulus. This is caused by the size and density difference between cutting particles, which is common in horizontal and highly inclined wells.
	Saltation	Cuttings are suspended but densely populated near the low-side wall so that it is virtually transported by jumping forward or saltating on the surface of the low-side wall.
	sand clusters	Cuttings are aggregated to clusters and transported together, where the velocity in clusters are roughly the same.
Rolling	Seperated moving bed	Separated sand beds are formed on the low-side wall of the annulus.
	continuous moving bed	A thin, continuous sand bed is formed on the low-side wall of the annulus with the sand near the low-side wall rolling or sliding forward at a lower velocity than that above the bed.
	stational bed	A continuous sand bed is formed on the low-side wall of the annulus with the sand on the surface of the bed rolling or sliding forward whilst the sand inside the bed is stationary.

The MTV will of course be dependent on all of the parameters which affect slurry transport: rheological properties of drilling fluids, hole angle, drill pipe eccentricity, annular fluid velocity, cuttings size etc. (Ford et al., 1990). Bello & Oyeneyin (2016) also found that the MTV was also greatly influenced by the above flow patterns. Most of the work done and reported in the literature for the minimum suspension velocity of solids in conduits is for

the pipe geometry because this is the geometry used for solids transport using liquids (mainly water) (Kelessidis and Bandelis, 2004; Govier and Aziz, 1972; Bagnold, 1957). Various models and correlations are developed to estimate the minimum transport velocity (MTV) in horizontal, inclined, and vertical well annulus. These studies can be generally classified as (1) empirical approaches and (2) theorical approaches. To satisfy the HDD features, which includes horizontal and highly inclined well and relatively large annular space, several models are introduced in the following.

2.7.2 Skalle's model

P. Skalle (2011) raised a mechanistic model for particles movement in inclined wells including hydraulic and mechanical forces. Figure 2.6 (Skalle, 2011) shows the forces involved in his model.

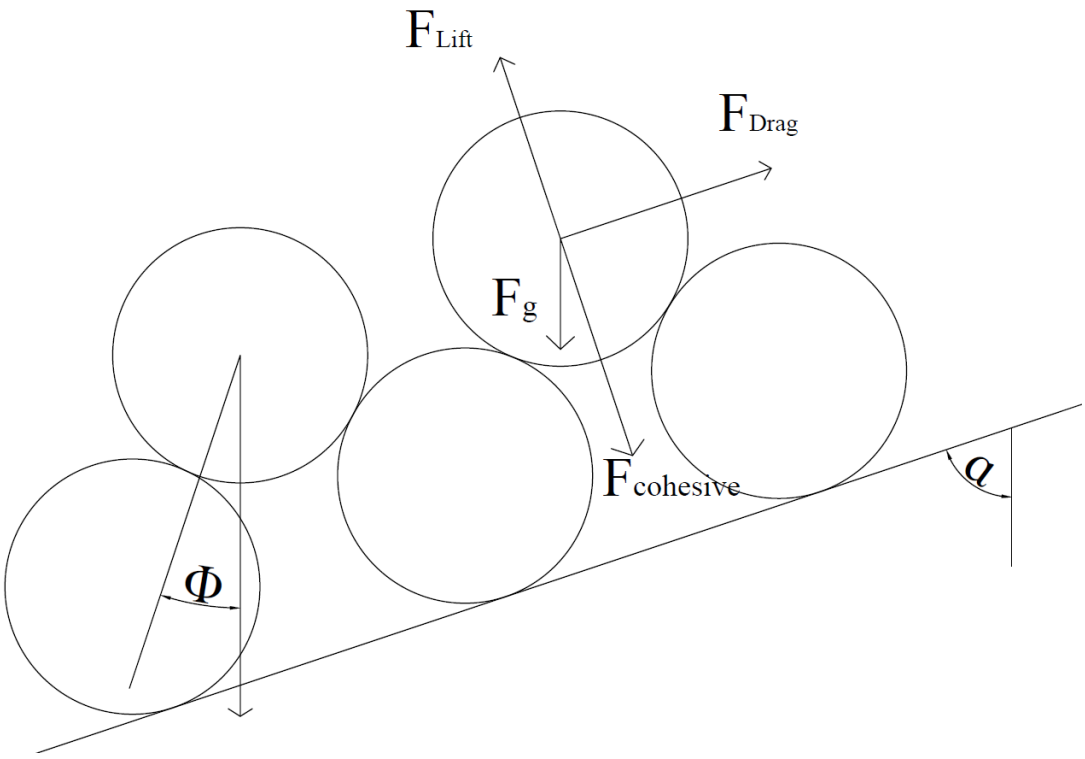

Figure 2.6 Force acting on the cutting particles on the cuttings bed (Skalle, 2011).

Main forces involved in cuttings transportation are drag force, lift force, cohesive force, and gravity force. Cohesive force is a force of attraction between particles in the mud and the bed and is classified as: (1) Attraction forces without contact consist of van der Waals forces and electrostatic forces. (2) Attraction forces with contact consist of viscous bridges or solid bridges (Skalle, 2011).

To lift the particles from cuttings bed and suspend particles in drilling fluid, Skalle (2011) raised a force balance equation 2-3

$$F_{net,lift} = F_{Lift} - F_{cohesive} - F_g * sin\alpha > 0 \quad (2\text{-}3)$$

To allow the particles to roll along the cuttings bed, another equation 2-4 is built:

$$F_{net,rolling} = \frac{d_p}{2}[F_D * sin\varphi + (F_{Lift} - F_{cohesive}) * cos\varphi + F_g * sin(-\alpha - \varphi)] > 0 \quad (2\text{-}4)$$

The symbols are defined below:

F_{Lift}: Lift force, kPa

$F_{cohesive}$: Cohesive force, kPa

F_g: Gravity force, kPa

F_D: Drag force, kPa

d_p: Diameter of particles, m

α: Cutting bed slope, degree

φ: Interaction angle between particles, degree

Skalle's theorical equations describe cuttings transport in ideal conditions, while in real project they may face many difficulties. The shapes of cuttings are usually irregular and interaction angle between particles is hard to measure. Some influential factors are not considered either, such as rheological properties of drilling fluid, etc.

2.7.3 Boyun's model

Boyun Guo (2013) also developed a theorical model for minimum mud flow rate. His

model estimates the minimum flow velocity in the vertical well by the formula 2-5:

$$V_{min} = V_{sl} + V_{tr} \tag{2-5}$$

, where V_{sl} is the particle slip velocity (m/s) and V_{tr} is the transport velocity.

The particle slip velocity is expressed as

$$V_{sl} = 2.79 * \sqrt{\frac{d_s}{f_p} * \left(\frac{\rho_s - \rho_f}{\rho_f}\right)} \tag{2-6}$$

The symbols are defined below:

d_s: Equivalent cuttings diameter, m

ρ_s: Cuttings density, kg/m^3

ρ_f: Fluid density, kg/m^3

f_p: Particle friction factor

The required transport velocity is expressed as

$$V_{tr} = \frac{\pi * d_b^2}{4 * C_P * A} * \left(\frac{ROP}{3600}\right) \tag{2-7}$$

The symbols are defined below:

d_b: Bit diameter, m

C_p: Cuttings concentration (volume fraction)

A: Annulus cross-sectional area at the certain depth, m^2

ROP: Rate of penetration, m/hr

The minimum flow rate in inclined well will be 1.8 times minimum flow velocity in vertical well. Regarding horizontal well, the minimum flow rate will be 1.5 times that in vertical well. In this case, his theorical model is also workable for horizontal and inclined well.

However, his model was mainly designed for drilling fluid which is Newtonian fluids and only provides conservative estimates for cuttings slip velocity in non-Newtonian fluids. In HDD drilling, the drilling fluid is comprised of water, bentonite and various additives, which is non-Newtonian fluids. As a result, the calculated minimum velocity by Boyun's model may be not precise enough.

2.7.4 Mitchell's model

Bill Mitchell (1995) raised another model for minimum flow velocity in the inclined well. His model is comprised of particle slip velocity and critical transport velocity showing below:

$$V_{min} = V_s * cos\varphi + V_t * sin\varphi \quad (2\text{-}8)$$

, where the V_s is the particle slip velocity (ft/min), V_t is the critical transport velocity (ft/min) and φ is the hole inclination angle (degree).

The particle slip velocity in the vertical well is expressed as:

$$V_s = 346.6 * \left[\frac{d_c^{1.6} * (\rho_s - \rho_f)}{\mu_e^{0.6} * \rho_f^{0.4}}\right]^{0.71} \quad (2\text{-}9)$$

The symbols are defined below:

d_c: Cuttings diameter (in)

μ_e: Effective viscosity (cp)

ρ_f: Drilling fluid density (ppg)

ρ_s: Drilling cuttings density (ppg)

The critical slip velocity in the vertical hole is expressed as:

$$V_h = 98.2853 * \left[\left(\rho_s - \rho_f\right) * \frac{(H-d)^3}{\rho_f}\right]^{0.16667} \quad (2\text{-}10)$$

The symbols are defined below:

ρ_f: Drilling fluid density (ppg)

ρ_s: Drilling cuttings density (ppg)

H: Hole diameter (in)

d: Drill pipe outer diameter (in)

Mitchell's model estimated the minimum annular fluid velocity for full cuttings transport

in inclined hole, which considered the multiple factors including inclination angle, cuttings size, drilling fluid rheological properties, etc. His model fits HDD features in some ways, but the critical velocity V_h is obtained based on the transport of large solids by a Newtonian liquid within a horizontal annulus. In HDD, drilling fluid is normally performed as non-Newtonian liquid.

2.7.5 Ozbayoglu et al. model

M.E. Ozbayoglu, A. Saasen, M. Sorgun and K. Svanes (2010) developed an empirical model based on a series of data from flow loop. Their model covered various factors including inclination angle, borehole diameter, rate of penetration, viscosity and density. The critical flow velocity is expressed as:

$$v_{crt} = 3.9835 * (\theta^{0.0378} * D_0^{0.4686} * ROP^{0.2343} * (D_0 + D_i)^{-0.2343} * \mu^{0.1137} * (D_0 - D_i)^{-0.022} * \rho^{-0.1137}) \quad (2\text{-}11)$$

The symbols are defined below:

v_{crt}: Critical flow velocity (ft/s)

θ: Inclination angle (degree)

D_0: Borehole diameter (in)

ROP: Rate of penetration (ft/hr)

D_i: Drill pipe diameter (in)

μ: Viscosity (cp)

ρ: Drilling fluid density (ppg)

However, their equation did not consider the cuttings characteristic and drilling fluid non-Newtonian behavior, which may not be precise enough for HDD.

2.7.6 Larsen et al. model

T.I Larsen, A.A. Pilehvari and J.J. Azar (1997) developed an empirical model to calculate critical transport flow velocity (CTFV) for high-angle wellbores and horizontal wells. Their model covered a series of correlation factors for cutting size, cutting concentration, drilling fluid density and inclination angles. Their experimental study focused on the annular fluid velocity needed to prevent cuttings from depositing in the wellbore (Larsen et al., 1997). Hole angle has a strong effect on hole cleaning efficiency (Shadizadeh and Zoveidavianpoor, 2012). Their design investigated the CTFV in highly inclined angles between 55 degrees and 90 degrees from vertical, which is well fitted for HDD feature. At or above the critical transport flow velocity calculated with Larsen et al.'s model, cutting bed will not form in the lower side of the borehole. On the other hand, their model estimated the MTV for suspension. As their experiments were conducted based on their experimental conditions, an additional correction factor of hole size for CTFV predictions is suggested

for different hole sizes. Jalukar et al. (1996) conducted a series of experiments to investigate the effect of hole size on cutting transport velocity, as an add-on for Larsen (1997) work. For hole angle greater than 45 degrees from vertical, as the hydraulic diameter increases, critical cuttings transport velocity requirement increases linearly (Jalukar et al., 1996).

According to Larsen et al.'s paper, the CTFV was comprised of Cuttings Transport velocity (CTV) and Equivalent Slip Velocity (ESV).

$$V_{crit} = V_{cut} + V_{slip} \tag{2-12}$$

The Cuttings Transport Velocity (CTV) can be calculated by:

$$V_{cut} = \frac{ROP}{36*\left[1-\left(\frac{D_{pipe}}{D_{hole}}\right)^2\right]*\left(0.64+\frac{18.16}{ROP}\right)} \tag{2-13}$$

The symbols are defined below:

ROP: Rate of Penetration (ft/hr)

D_{hole}: Diameter of the borehole (in)

D_{pipe}: Diameter of the drilled pipe (in)

The Equivalent Slip Velocity (ESV) can be calculated by:

$$\bar{V}_{slip} = \begin{cases} 0.00516 * \mu_a + 3.006, & \mu_a < 53\ cp \\ 0.02554 * (\mu_a - 53) + 3.28, & \mu_a > 53\ cp \end{cases} \tag{2-14}$$

, where μ_a is the apparent viscosity (cp)

Larsen applied several modification coefficients considering the inclination angle, cuttings size and mud-weight. The modified slip velocity is calculated by

$$V_{slip} = \bar{V}_{slip} * C_{ang} * C_{size} * C_{mwt} \quad (2\text{-}15)$$

Jalukar et al. established a series of hole geometry correction factor for hole diameter, rheology and angle to T.I Larsen, A.A. Pilehvari and J.J. Azar's model. Larsen's critical cuttings transport velocity is modified as the formula showing below:

$$V_{CRIT(Corr)} = V_{CRIT} * C_{Geo(D)} * C_{Geo(PV)} * C_{Geo(\theta)} \quad (2\text{-}16)$$

If the flow velocity in the annulus is lower than the CTFV, the drilled particles will settle down in the lower side. Cuttings bed could grow and narrow the borehole cross-section. The development of cuttings bed will not stop until the produced cuttings equal to removed cuttings, for that the drilling fluid flow velocity increases with the decreasing cross-section area. The drilling rate and drilling fluid flow rate are the most important factors controlling the formation of stationary the cuttings bed (Bjorndalen and Kuru, 2004).

Larsen's model considered both drilling rate, drilling fluid flow rate and a series of significant factors including drilling fluid apparent viscosity, inclination angle, borehole diameter, etc. Although his model was originally designed for drilling in oil and gas well, it satisfied the mini-HDD or pilot hole stage of Midi/Maxi-HDD features as well, which

may be suitable for estimating the minimum drilling fluid velocity in the borehole.

2.7.7 Conclusion

Five minimum required flow velocity models designed for horizontal and highly inclined well are introduced and discussed. Each model has its unique features and restrictions. Skalle's model was designed for ideal conditions, while some parameters in the model could not be measured or estimated. Boyun's model was designed for Newtonian drilling and only provided conservative estimates for cuttings slip velocity in non-Newtonian fluids. Mitchell's model partially considered the non-Newtonian behaviors of drilling fluid and highly inclined borehole, but the critical transport velocity in the model is calculated based on Newtonian drilling fluid. Ozbayoglu's model was an empirical model which covered various parameters but ignored the cuttings characteristic and drilling fluid non-Newtonian behavior. Larsen's model with Jalukar's corrections considered almost all significant parameters related to cuttings transport and the unique features of HDD, such as highly inclined borehole and non-Newtonian behavior drilling fluid. Overall, based on the features of the above models, Larsen's model fits the HDD features well, which is likely to get the best estimation of minimum required velocity in mini-HDD project. Furthermore, more experiments and data may be needed to compare the accuracy of these models.

2.8 Maximum Flow rate

Expect for the clogging in the annulus, there are two main failure mechanisms that can

occur during an HDD: shear and tensile (Balcay and Baser, 2019). The first mechanism is associated with generalized shear failure which generates unconfined plastic flow in surrounding soil, so called "blowout," e.g. (Arends, 2003; Balcay and Baser, 2019). Tensile failure usually refers to hydro fracture, which is a specific occurrence in non-fissured cohesive soils when the pressure of the drilling fluid exceeds the strength and confining stress of the surrounding soils and the excess pressure fractures the soil around the bore, allowing the drilling fluids to escape the annulus (Bennett and Wallin, 2008). Both phenomena are affected by the pressures of the drilling mud used to stabilize the excavated zone, which finally lead to the control of drilling fluid flow rate. High flow rate will raise the borehole annular pressure and further increase the risk of hydraulic failure (Deng, 2018).

2.8.1 Borehole annular pressure estimation

The first step of HDD (pilot boring) has the greatest construction concern due to the high risk of hydraulic fracture and loss of drilling fluid circulation (Rostami, 2017). It is recommended that the developments for monitoring the key operational parameters continue and that available systems are implemented, which should include the drill fluid pressure in the borehole (Keulen, 2001). Planning and measuring annular pressure are crucial for large scale HDD projects and serves as a diagnosis tool during drilling (Murray et al., 2014). It is also important that more down-hole pressure data be collected and compared with cavity expansion predictions where inadvertent returns occur so that we may gain a better understanding of the plastic zone behavior (Staheli, 2010). In HDD

project, the quantitative HDD dataset contains real-time annular pressure measurements that were recorded using an annular pressure tool, which is located in the bottom hole assembly (BHA) directly behind the drill bit and mud motor (Murray et al., 2014).

Prior to measuring the annular pressure during construction, annular pressure could be divided into two pressure components within the borehole, including the hydrostatic pressure and the friction loss pressure (Murray et al., 2014). The annular pressure could be calculated as:

$$P = P_s + P_f \tag{2-17}$$

The hydrostatic pressure depends on drilling fluid density and borehole depth. It could be calculated as (Mitchell and Miska, 2011):

$$P_s = \rho * g * \Delta Z \tag{2-18}$$

The symbols are defined below:

P_s refers to hydrostatic pressure (Pa).

ρ refers to density of drilling fluid, including the produced cutting (kg/m^3).

g refers to the acceleration of gravity (N/kg).

ΔZ refers to elevation difference (m) between the drill rig entry point and the point of interest within the bore as far as the desired point is located below the entry point; otherwise,

the hydrostatic pressure is zero (Rostami, 2017).

The frictional pressure loss depends on the fluid properties, the flow velocity, the flow regime, and the length of the flow path (Guo and Liu, 2011). In HDD the large annular space and limited pump pressure, as well as the high risk of hydro fracture all, imply that pumping drilling fluids, even water, in turbulent flow is impractical (Deng, 2018; Shu et al. 2015). As a result, drilling fluid in the annulus is usually considered as laminar flow in horizontal directional drilling. Different rheological models including Newtonian, Bingham plastic, and power-law model can be employed to develop the mathematical relation between flow rate and frictional pressure drop (Mitchell and Miska, 2011). The drilling fluid is usually formed by water, bentonite, and additives, which will not perform as Newtonian fluid. Bingham plastic and power-law model are widely used in HDD project. Their shear stress-shear rate relationships of the three rheological models are showing below:

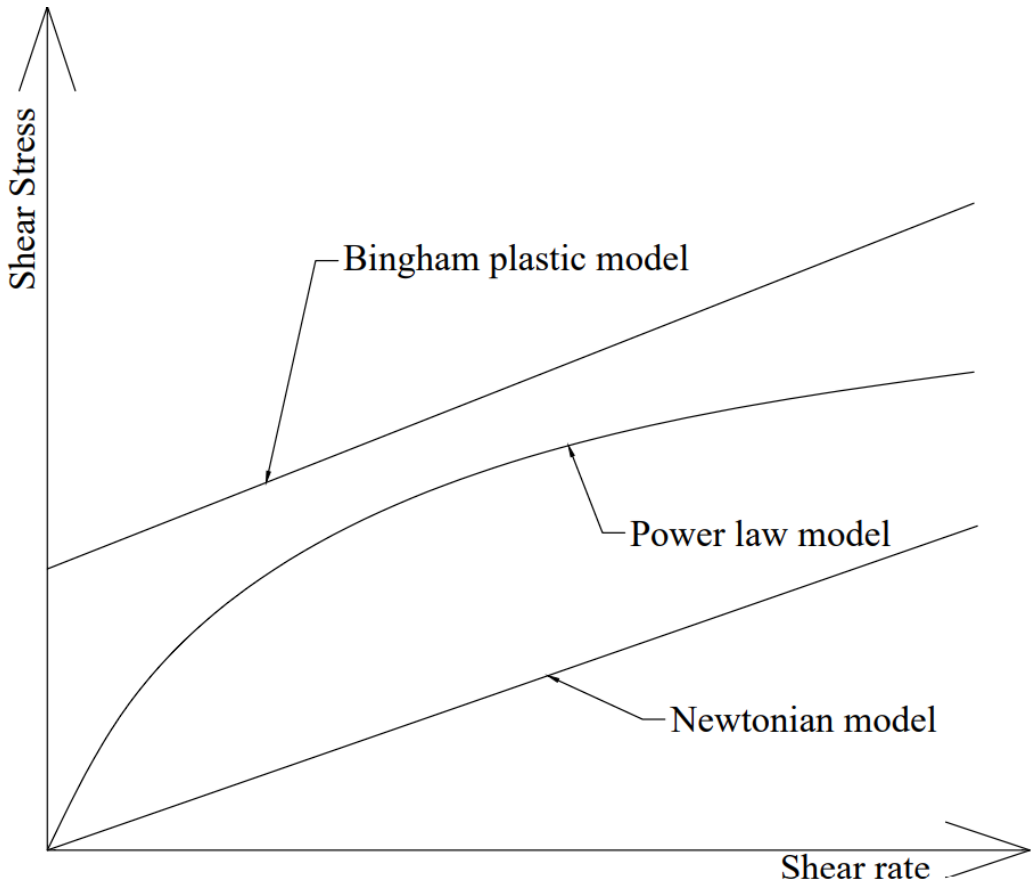

Figure 2.7. Bingham plastic model and Power law model

The Bingham plastic Model has a linear relationship between shear rate and shear stress, which is the simplest rheological model and assumes true plastic behavior (Ariaratnam, 2003). It is a 2-parameter model and easily used in Horizonal Directional Drilling project. Its equation is shown below:

$$\tau = \tau_y + \mu_p * \gamma \tag{2-19}$$

The symbols are defined below:

τ_y: Yield point (stress) (Pa), could be calculate from $\theta_{300} - \mu_p$

μ_p: Plastic viscosity (Pa*s), could be calculated from $\theta_{600} - \theta_{300}$

τ: Shear stress (Pa)

γ: Shear rate (/s)

θ_{600}, θ_{300}: Dial reading of rheometer at 300 and 600 RPM

For drilling muds, this model does not accurately describe the mud's behavior at low shear rates (Guo and Liu, 2011). But Rostami (2017) argued that Bingham Plastic model are normally used to predict annular pressure at shear rates of 300-600 RPM, which provides a conservative estimate and promotes deeper and longer drill paths at design phase, requiring unnecessary installation expense. To modify the suggested rheological model (Bingham plastic model) by HDD industry to estimate the annular pressure during pilot boring, a new shear rate ranges are introduced as 100-200 RPM which can provide a most favorable agreement with the annular measurements (Rostami, 2017).

According to Mitchell and Miska (2011), the frictional pressure loss gradient for the laminar flow in the annulus can be calculated by Equation 2-20, with the Bingham Plastic model:

$$\frac{dP_f}{dL} = \frac{48 * \mu_p * v}{(D_B - D_{DP})^2} + \frac{6 * \tau_y}{D_B - D_{DP}} \qquad (2-20)$$

Solving the flow rate at this frictional pressure loss,

$$Q = \frac{\pi}{192 * \mu_p} * \frac{dP_f}{dL} * ({D_B}^2 - {D_{DP}}^2) * (D_B - D_{DP})^2 - \frac{\pi}{32 * \mu_p} * \tau_y * ({D_B}^2 - {D_{DP}}^2) * (D_B - D_{DP}) \quad (2-21)$$

In the drill path with length L, the frictional pressure loss can be calculated as:

$$P_f = \left(\frac{48 * \mu_p * v}{(D_B - D_{DP})^2} + \frac{6 * \tau_y}{D_B - D_{DP}}\right) * L \quad (2-22)$$

The symbols are showing below:

P_f: Annular frictional pressure loss (Pa).

D_B: Diameter of the borehole (m).

D_{DP}: Diameter of the drill pipe (m).

v: Average velocity (m/s)

L: Drill path length (m)

Power law model

The Ostwald-de-Waele or Power Law model describes the shear-thinning behavior of drilling fluid. It is also a 2-parameter model, and its equation is calculated as:

$$\tau = k\gamma^n \quad (2\text{-}23)$$

The symbols are showing below:

k: Consistency index related to viscosity of the fluid ($\frac{dyne*sec^n}{cm^2}$)

n: Power Law exponential index

Considering the shear thinning behavior of drilling fluids, the n value should be assumed between zero and one (Rostami, 2017; Baroid, 1997). The estimation compared to measured annular pressure in different case studies showed that, the Power Law model can provide a good estimation of annular pressure and can be recommended to the HDD industry for annular pressure estimation (Rostami, 2017).

According to Mitchell and Miska (2011), the frictional pressure loss gradient for the laminar flow in the annulus can be calculated with Power law model as:

$$\frac{dP_f}{dL} = \frac{4 * k * \left(8 + \frac{4}{n}\right)^n * v^n}{(D_B - D_{DP})^{n+1}} \qquad (2-24)$$

Solving the flow rate at this frictional pressure loss,

$$Q = \frac{\pi \left(\frac{1}{k} * \frac{dP_f}{dL}\right)^{\frac{1}{n}}}{2^{3+\frac{2}{n}} * \left(4 + \frac{2}{n}\right)} * ({D_B}^2 - {D_{DP}}^2) * (D_B - D_{DP})^{1+\frac{1}{n}} \qquad (2-25)$$

In the drill path with length L, the frictional pressure loss can be calculated as:

$$P_f = \frac{4 * k * \left(8 + \frac{4}{n}\right)^n * v^n}{(D_B - D_{DP})^{n+1}} * L \qquad (2-26)$$

The symbols are showing below:

P_f: Annular frictional pressure loss (Pa).

D_B: Diameter of the borehole (m).

D_{DP}: Diameter of the drill pipe (m).

v: Average velocity (m/s)

L: Drill path length (m)

In general, all equations could be summarized in the table 2.5:

Table 2.4. Calculations of frictional pressure gradient, frictional pressure loss and flow rates with Bingham Plastic model and Power Law model

Rheological Model	Bingham Plastic model	Power Law model
Equation	$\tau = \tau_y + \mu_p * \gamma$	$\tau = k\gamma^n$
Frictional Pressure Gradient	$\frac{dP_f}{dL} = \frac{48 * \mu_p * v}{(D_B - D_{DP})^2} + \frac{6 * \tau_y}{D_B - D_{DP}}$	$\frac{dP_f}{dL} = \frac{4 * k * \left(8 + \frac{4}{n}\right)^n * v^n}{(D_B - D_{DP})^{n+1}}$

Frictional Pressure loss	$P_f = \left(\frac{48 * \mu_p * v}{(D_B - D_{DP})^2} + \frac{6 * \tau_y}{D_B - D_{DP}}\right) * L$	$P_f = \frac{4 * k * \left(8 + \frac{4}{n}\right)^n * v^n}{(D_B - D_{DP})^{n+1}} * L$
Flow Rates	$Q = \frac{\pi}{192 * \mu_p} * \frac{dP_f}{dL} * ({D_B}^2 - {D_{DP}}^2) * (D_B - D_{DP})^2 - \frac{\pi}{32 * \mu_p} * \tau_y * ({D_B}^2 - {D_{DP}}^2) * (D_B - D_{DP})$	$Q = \frac{\pi \left(\frac{1}{k} * \frac{dP_f}{dL}\right)^{\frac{1}{n}}}{2^{3+\frac{2}{n}} * \left(4 + \frac{2}{n}\right)} * ({D_B}^2 - {D_{DP}}^2) * (D_B - D_{DP})^{1+\frac{1}{n}}$

2.8.2 Maximum borehole pressure

New techniques have been developed to monitor drilling mud pressures in the field, but further work is still needed to quantify the maximum allowable mud pressure that leads to hydrofracturing or blowout especially when drilling through sand (Xia, 2009). Maximum allowable drilling fluid pressure is defined as the maximum pressure that soil can sustain without failure during horizontal directional drilling (Balcay and Baser, 2019). When the pressure in the borehole exceeds the strength of surrounding strata, a frac-out condition occurs in which drilling fluid escapes from the borehole and migrate to the surface (Ariaratnam et al., 2003).

The first model applied to predict the maximum allowable pressure following shear failure assumption was proposed by Luger and Hergarden in 1988, which is later known as Delft's solution (Rostami, 2017). It was used to calculate a maximum allowable pressure for a given soil mass based upon bore geometry, engineering properties of the soil mass, and an assumed influence zone surrounding the bore (Andresen and Staheli, 2019). The solution was originally developed from Expansion of cavities in infinite soil mass raised by Vesic in 1972. It is considered to be the state-of-the-art practice by the U.S. Army Corps of Engineers-USACE (Carlos et al., 2002).

The maximum annular pressure, defined by Luger and Hergarden in 1988, could be calculated as:

$$P_{max} = u + [\sigma_0' * (1 + sin\varphi) + c * cos\varphi + c * cot\varphi]$$
$$* \left(\left(\frac{R_0}{R_{pmax}} \right)^2 + \frac{\sigma_0' * sin\varphi + c * cos\varphi}{G} \right)^{\frac{-sin\varphi}{1+sin\varphi}} - c * cot\varphi \qquad (2-27)$$

The symbols are defined below:

P_{max} refers to maximum allowable pressure in the annulus (Pa).

u refers to initial in-situ pore pressure (Pa).

φ refers to friction angle of soil (degree).

R_0 refers to borehole radius (m).

G refers to shear modulus (Pa).

c refers to cohesion coefficient (Pa).

R_{pmax} refers to the plastic zone. A factor of safety (FoS) may be applied (m).

σ_0' refers to effective stress (Pa) which is dependent on depth and soil conditions, defined by $\gamma * (h_{tot} - h_w) + \gamma' * h_w$

The assumption and discussion of this equation could be summarized in Table 2.4 (Andresen and Staheli, 2019).

Table 2.5. Multiple assumptions in Delft Equation (Andresen and Staheli, 2019).

Assumption	Add-on to Delft Equation
The cylindrical cavity is axially symmetric, which could expand in infinite space without boundary	Delft equation is more accurate in deeper boreholes, as constant pressure distribution is approximately uniform with large cover depth .
The borehole and confining pressures attain static equilibrum	This assumption describe that the confining and expanding pressure are at constant equilibrium. To fit this assumption, Delft Equation could have better performance in a) a borehole condition with a well-established filter cake and b) clayey soils with low permeability which do not readily allow flow. However, the equation do not apply to dynamic loading.
The soil medium is considered as homogenous and isotropic material	Geologic conditions are rarely homogenous or isotropic near surface, due to the roots, utilitues, piles, and other fissures. The surface loading such as road compaction, building loads and other activities could change the soil parameters. In deep locations within native soil deposits, soil conditions are more likely to be homogenous and isotropic.
The elastic stress obeys Hook's law and elastic is neglected in the plastic zone	Coarse frained soils tend to display elastic stress strain behavior with recoverable strain when subjected to small displacements. While saturated soils are likely to display time dependent behavior.
The soil stress is defined by Mohr-Coulomb failure criteria	The Mohr-Coulomb failure criterion assumes that the cohesion and internal frictional angle are constant with depth, which is suitable for soils analysis. It could be more applicable if the estimated the cohesion and friction angle in lab was performed at similar stress levels to the designed field values
No volume change exacts in the plastic zone	This is a common assumption in soil mechanics.

Van and Hergarden (1997) suggested that the maximum allowable pressure of the soil is limited to extension of the plastic radius to half of the way to ground surface in purely cohesive soil and to two thirds of the way in frictional soils (Rostami, 2017).

Keulen (2001) extended the work of Lugar and Hergarden (1997) by conducting laboratory experiments designed to determine the effectiveness of their assumptions (Xia, 2009). Keulen (2001) concluded that L&H's model had the possibility to introduce dilatancy in

the plastic region. Keulen (2001) suggested that parameters in the model can be determined from simple soil investigation and by engineering judgement, but also reminded there were lots of uncertainties (i) in the models used, (ii) the parameters that are filled in, (iii) and in the measured values.

The Delft solution considers generalized shear failure in the plastic zone of the soil surrounding the borehole, Xia and Moore (2006) considered tensile failure of the soil upon exceeding the minor principal stress (Murray et al., 2014). Xia (2009) did series of finite element analysis of small-scale and large-scale laboratory test, which provided an effective calculation of the maximum mud pressure value. Xia (2009) concluded that Delft solution neglects the effect of lateral earth pressure at rest K_0, the ground surface and gradient of strength and stress with depth, therefore overestimated the maximum allowable mud pressure by 160% to 180%. A safety factor of at least 2.5 is suggested based on these comparisons if calculating maximum mud pressure using the Delft solution, however, this safety factor still depended on the field conditions such as soil characteristics, initial stress condition and so on, good engineering judgment and geotechnical experience were needed when designing pipeline installation using the Delft solution (Xia, 2009).

Staheli (2010) conducted a series of sensitivity analysis for cavity expansion theory and concluded that the use of the maximum pressure calculation by delft equation overestimates actual pressure at which inadvertent returns occurred when using large values of R_{pmax}. Maximum pressure is only sensitive to R_{pmax} in the initial portion of

the curve, upon achieving 90% of the ultimate value, relatively large changes in R_{pmax} have only minor impact upon maximum pressure (Andresen and Staheli, 2019). The accuracy of the predicted maximum pressure could be improved by calculating the maximum allowable pressure when R_{pmax} is very small (on the order of 2-3 bore-hole diameters or less) or applying a factor of safety to the maximum borehole pressure with R_{pmax} calculated at the ground surface (Staheli, 2010).

Rostami (2017) concluded that an increase in overburden pressure led to a decrease in plastic radius on set of failure and the limited pressures calculated were higher than the measured failure pressures due to the assumption of uniform expansion to infinity. Rostami's parametric study confirmed that the parameters of overburden depth, friction angle, and elastic modulus of the soil medium have the highest impact on the failure pressure.

As a result, there are three components to effectively using a tool such as the Delft equation to successfully model the borehole conditions during drilling: 1) a thorough understanding of the model assumptions, sensitivity, and contribution of the input parameters, and any empirical components, 2) understanding of geotechnical principals necessary to apply the model to a complex three phase matter with appropriate conservatism, and 3) understanding of the field conditions and if one or more of the assumptions upon which the model is based are not met (Andersen and Staheli, 2019).

There are some other close form and analytical solutions which are barely used in HDD and are formulated based on cavity expansion solution (Rostami, 2017). Yu and Houlsby (1991) presented a unified analytical solution for the stress and displacement for the expansion of both cylindrical and spherical cavities, considering the dilatancy of the soils. The summary of cavity expansion model was detailly introduced in Yu's book Cavity Expansion Methods in Geomechanics. However, when extending the limit pressure solution to estimate the maximum allowable pressure during HDD, the limit pressure calculated based on Yu and Houlsby's solution overestimated the failure pressure significantly (Rostami, 2017).

What's more, some papers (Kennedy et al, 2004; Xia, 2009; Lan and Moore, 2018; Lan and Moore, 2022) did not agree on Delft Equation. Kennedy et al (2004) used elastic finite element analysis to estimate the maximum allowable drilling fluid pressure during HDD based on elastic plate theory. Kennedy (2004) mentioned that the reason why the Delft equation provided unconservative estimates of limiting pressure is likely because it assumed the initial earth pressure is isotropic (the coefficient of lateral earth pressure is 1). Lan and Moore (2018) identified new criteria for identifying tensile failure versus shear failure, instead of calculating the maximum allowable mud pressure when drilling in saturated clay. They also investigated a new numerical design equation for mud pressure in 2022.

Although some different solutions were developed in the past 30 years, and researchers

haven't reached a common agreement on Delft Equation, Delft Equation is still accepted by many researchers (Neher, 2013; Staheli et al., 2010; Andresen and Staheli, 2019; Rostami et al.; 2015) and widely used in HDD industry. As a result, this paper still uses the Delft Equation to estimate the maximum drilling fluid allowable pressure in HDD.

2.9 Conclusion

This chapter provided an overview of the drilling fluid studies with flow rate annular pressure in HDD. The drilling fluid flow regime and angle of inclination were also discussed. Due to the considerable risk of stuck pipe in the pilot boring stage, minimum flow rate and critical flow velocity (minimum transport velocity) were introduced to estimate the lower boundary of drilling fluid flow rate. On the other hand, maximum allowable pressure in the annulus were illustrated to design maximum flow rate. Based on the discussion showing above, some characteristics of drilling fluid could be concluded:

(1) HDD borehole has relative larger diameter, compared with wells in petroleum engineer. Considerable borehole diameter limited the drilling fluid flow regime to laminar flow, although turbulent flow has better performance in hole cleaning, compared with laminar flow.

(2) Developed from oil and gas engineering, HDD has some unique features, including highly inclined and horizontal borehole, shallow cover depth and water-based drilling fluid. Minimum flow velocity models used in oil and gas engineering more or less have

some defects. Of five different models, Larsen's model provided the best accuracy for the minimum flow velocity predictions.

(3) Annular pressure is comprised of hydrostatic pressure and frictional pressure loss. Hydrostatic pressure is proportional to drilling fluid density and cover depth, while frictional pressure loss is related to drilling fluid rheological properties, flow rate and borehole length.

(4) Hole cleaning performance could be significantly improved by increasing the annular flow rates. However, annular frictional pressure loss will also increase with the raising flow rate. On the other hand, frictional pressure loss induced by drilling fluid limits the increase of the flow rate in the annulus.

(5) Delft solution is widely used to determine the maximum allowable pressure in the annulus. To have a conservative estimate with Delft Solution, the plastic zone may be chosen as 2 – 3 borehole diameters or additional factor of safety may be added in final calculations.

Chapter 3: Feasibility of Larsen's model for minimum drilling fluid velocity in HDD pilot boring stage

3.1 Introduction

During the past few years, trenchless technologies have been gaining popularity in the area of buried infrastructure rehabilitation due to economic and environmental factors (Moteleb and Salem, 2004). Trenchless technology refers to a variety of underground construction methods that require minimal trenching or surface disruption, which require sinking one or several shafts, but eliminates the need for continuous open trenches (Dayal, et al., 2011). Compared with traditional open cut method, various disadvantages of open cut method could be avoided by adopting trenchless technology (Gunjal, 1996):

- Traffic hindrance, traffic obstruction, accidents, providing diversions and their maintenance.

- Environmental pollution, dust and air pollution by vehicles and machines, noise pollution, ground and surface water pollution, etc.

- Loss to commerce and industry due to reduced sales, low productivity, increased consumption of petrol, oil and lubricants.

- Possible avoidable cost in repair and rehabilitation roads, compensation for damage, disadvantage of early availability of utility and public hindrances.

Among various trenchless technologies, more than 70% of all underground installations in the world are done by HDD (Gerasimova, 2016). HDD is a technique used to install an underground infrastructure (pipelines, water supply systems, sewerage, and power lines) by overcoming natural or artificial obstacles such as streets, buildings, railways, rivers, and lakes (Tervydis and Jankuniene, 2017). HDD combined the technologies from different industries including utility, oil field and water well industries. In the past decade, this disproportionate growth in the HDD market – in comparison to other branches of civil engineering – has led to HDD suddenly being offered by a large range of companies (Bernhard and Gerhard, 2008).

However, in the HDD drilling process, hole cleaning is always one of the most common and costly problems, which is also an issue in conventional oil well drilling (Sai, 2018; Osbak 2012; Pilehvari et al. 1999). Insufficient hole cleaning affects the penetration rate, and consequently, causes fluid loss, lost circulation, and stuck pipe (Mohmoud et al., 2020). The major parameters which affect hole cleaning in the wellbore rely on different parameters such as: drilling fluid flow rate, angle of inclination, rate of penetration, yield point, plastic viscosity, cutting size, rate of penetration (ROP), etc. (Busahmin et al., 2017). It could be generally classified into three groups: (1) fluid parameters, such as flow velocity, mud density, and rheological properties; (2) cutting parameters, such as cuttings density, dimension, and concentration; (3) operational parameters, such as hole inclination (from vertical), rate of penetration as well as drill pipe rotation and eccentricity in the annulus

(Sai, 2018; Bilgesu et al. 2007). Among these influence factors in three groups, fluid flow velocity is the dominant drilling variable in hole cleaning due to its direct relation with the shear stress acting on the cuttings bed (Ozbayoglu et al., 2010; Kjosnes et al., 2003).

HDD industry developed a practical model to design drilling fluid flow rate for different projects, which is proportional to the cuttings production rate. Drilling engineering also developed different theorical and empirical model to design proper drilling fluid flow velocity in the wellbores. T.I. Larsen, A.A. Pilehvari and J.J. Azar developed a cuttings transport model for high-angle wellbores including horizontal wells in 1997. They investigated all variables believed to control the hole cleaning performance between the angles 55 degrees to 90 degrees from vertical in a 5-in. full scale flow loop. Their study covered the effect of inclination angle, rate of penetration (ROP), cutting size, drilling fluid density and rheological properties to the hole cleaning performance. Over 700 tests were conducted based on 5 types of drilling fluid with different rheological properties, 3 different cuttings sizes (0.275 in., 0.175 in., and 0.09in.) and 3 different cuttings injection rates (27, 54, and 81 ft/hr). Their model predicted the critical transport fluid velocity (CTFV) for removing cuttings bed in the wellbores and cuttings concentration when drilling fluid circulating velocity was slower than the CTFV. L.S. Jalukar, J.J. Azar, A.A. Pilehvari and S.A. Shirazi (1996) made a hole size correction factor for the CTFV predictions as a continuation of the model.

In this study, a case study about the horizontal wellbore with all necessary data was applied

to Larsen's model to obtain the critical transport fluid velocity (CTFV) and cuttings concentration. The calculated cuttings concentrations were used to fit the measured cuttings concentration from the case study. The accuracy of Larsen's model in predicting the cuttings concentration in small scale horizontal annulus were compared and discussed. Afterwards, the drilling fluid flow velocity designed by HDD industry method was also applied to Larsen's model to simulate the possible cuttings concentration in the annulus. The cuttings concentration results from HDD industry were evaluated and discussed.

3.2 Background

3.2.1 HDD industry estimation

The minimum flow rate in HDD project is proportional to the cuttings production rate, which could be calculated with the formula below:

$$Q_{fluid} = C_s * Q_c \tag{3-1}$$

The symbols are defined below:

Q_{fluid}: Drilling fluid flow rate (m^3/min)

C_s : Fluid-to-Soil ratio, depends on soil conditions (showing on Table 3.1)

Q_c: Cutting's production rate (m^3/min)

Table 3.1 Suggested Fluid-to-soil ratio (Vroom, 2018)

Soil	Factor of Safety (Drilling Fluid/cuttings)
Sand, Gravel, Cobble	1:1 or 2:1
Fine sand, clay-like sand	2:1 or 3:1
Sandy clay	3:1 or 4:1
Reactive clay	5:1 or more

The cutting's production rate is related to the cross-section area of the borehole, rate of penetration and soil conditions, which could be calculated from Mitchell and Miska's book (2011) with the formula below:

$$Q_c = A_{hole} * ROP * (1 - porosity) \quad (3\text{-}2)$$

The symbols are defined below:

A_{hole}: Cross section area of the borehole (m^3).

ROP: Rate of Penetration (m/h).

$porosity:$ Porosity of the soil.

3.2.2 Critical transport flow velocity (Larsen's method)

T.I Larsen, A.A. Pilehvari and J.J. Azar (1997) developed an empirical model to calculate critical transport fluid velocity (CTFV) for high-angle wellbores and horizontal wells.

Their critical transport fluid velocity CTFV is expressed as:

$$V_{crit} = V_{cut} + V_{slip} \quad (3\text{-}3)$$

, where V_{crit} is critical transport fluid velocity (CTFV) (ft/s), V_{cut} is Cuttings Transport velocity (CTV) (ft/s) and Equivalent Slip Velocity (ESV) (ft/s).

The Cuttings Transport Velocity (CTV) can be calculated by:

$$V_{cut} = \frac{ROP}{36 * \left[1 - \left(\frac{D_{pipe}}{D_{hole}}\right)^2\right] * \left(0.64 + \frac{18.16}{ROP}\right)} \quad (3-4)$$

The symbols are defined below:

V_{cut}: Cuttings transport velocity (CTV) (ft/s)

ROP: Rate of Penetration (ft/hr)

D_{hole}: Diameter of the borehole (in)

D_{pipe}: Diameter of the drilled pipe (in)

The Equivalent Slip Velocity (ESV) can be calculated as:

$$\bar{V}_{slip} = \begin{cases} 0.00516 * \mu_a + 3.006, & \mu_a < 53\ cp \\ 0.02554 * (\mu_a - 53) + 3.28, & \mu_a > 53\ cp \end{cases} \quad (3\text{-}5)$$

$\bar{V}_{slip}$ is the unmodified Equivalent Slip Velocity (ESV) (ft/s), μ_a is the apparent viscosity (cp), which can be calculated by:

$$\mu_a = \mu_p + \frac{5 * Y_p * (D_{hole} - D_{pipe})}{V_{crit}} \quad (3-6)$$

The symbols are defined below:

μ_p: Plastic viscosity, obtained from fann viscometer reading or Bingham Plastic model. (cp)

Y_p: Yield point, obtained from fann viscometer reading or Bingham Plastic model. (lbf/100ft^2)

As the critical flow velocity, which is the final result of the method, is needed to calculate the apparent viscosity, an iterative procedure is required. Multiple correction factors for inclined angle, cuttings-size, drilling fluid weight are applied to ESV. The Angle of Inclination Correction Factor could be calculated by:

$$C_{ang} = 0.0342 * \theta_{ang} - 0.000233 * \theta_{ang}^2 - 0.213 \quad (3\text{-}7)$$

Where the θ_{ang} is the angle of inclination of the borehole from vertical (degree).

The Cuttings-Size Correction Factor could be calculated by:

$$C_{size} = -1.04 * D_{50cut} + 1.286 \quad (3\text{-}8)$$

Where the D_{50cut} is the mean cuttings size (in).

Mud-Weight Correction Factor could be calculated by:

$$C_{mwt} = \begin{cases} 1 - 0.0333 * (\gamma_m - 8.7) & ,\gamma_m > 8.7 \\ 1 & ,\gamma_m < 8.7 \end{cases} \quad (3\text{-}9)$$

Where the γ_m is the desity of mud (Ibf/ gal).

With these factors, the generalized ESV could be calculated by:

$$V_{slip} = \bar{V}_{slip} * C_{ang} * C_{size} * C_{mwt} \quad (3\text{-}10)$$

Jalukar et al. established a series of hole geometry correction factor for hole diameter, rheology and angle to T.I Larsen, A.A. Pilehvari and J.J. Azar's model. Larsen's critical cuttings transport velocity is modified as the formula showing below:

$$V_{CRIT(Corr)} = V_{CRIT} * C_{Geo(D)} * C_{Geo(PV)} * C_{Geo(\theta)} \quad (3\text{-}11)$$

$C_{Geo(D)}$: Hole diameter correction factor.

$C_{Geo(PV)}$: Drilling fluid rheological factor.

$C_{Geo(\theta)}$: Angle correction factor.

The hole geometry correction factor for diameter $C_{Geo(D)}$ could be calculated as:

$$C_{Geo(D)} = 0.277 D_{hyd} + 0.2696 \quad (3\text{-}11)$$

Where D_{hyd} is Hydraulic diameters (in), in annulus which is expressed in $D_h - D_p$; D_h, D_p are the hole and drill pipe diameter (in).

The hole geometry correction factor for rheology $C_{Geo(PV)}$ could be calculated as:

$$C_{Geo(PV)} = -0.00205841 * \mu_p + 1.01493 \quad (3\text{-}12)$$

Where μ_p is the plastic viscosity of drilling fluid (cp).

The hole geometry correction factor for angle $C_{Geo(\theta)}$ could be calculated by the

following formula,

$$C_{Geo(\theta)} = 1.15667 * 10^{-5} * \theta^3 - 0.0026645 * \theta^2 + 0.200266 * \theta - 3.91019 \quad (3\text{-}13)$$

Where θ is borehole angle (rad).

For flow velocity below Larsen's critical cuttings transport velocity (CTFV), cuttings will start to deposit in the borehole. Larsen et al. assumed that the velocity in the open area above the cuttings bed will be equal to the CTFV when the cuttings bed stops growing or eroding. As a result, the cuttings concentration (C_{bconc}) or average cross-sectional area of the cuttings in the annulus, can be calculated by using the cuttings bed porosity (φ) in the following formula:

$$\overline{C_{bconc}} = 100 * \left(1 - \frac{Q_{pump}}{Q_{crit}}\right) * (1 - \varphi) \quad (3 - 14)$$

Where $\overline{C_{bconc}}$ is the cuttings concentration for a stationary bed (not corrected by drilling fluid apparent viscosity) (%), Q_{crit} is the critical transport flow rate (gpm), Q_{pump} is the pump flow rate (smaller than Q_{crit}) (gpm), φ is the cuttings bed porosity.

Correction Factor for Cuttings Concentration will also be applied to the cutting's concentration based on the apparent viscosity in Formula 3-15

$$C_{bed} = 0.97 - 0.00231 * \mu_a \quad (3\text{-}15)$$

Where C_{bed} is the correction factor for cuttings concentration, μ_a is the apparent

viscosity (cp)

Overall, the final cuttings concentration can be calculated by:

$$C_{bconc} = \overline{C_{bconc}} * C_{bed} \quad (3\text{-}16)$$

Where C_{bconc} is the cuttings concentration for a stationary bed (%), C_{bed} is the correction factor for cuttings concentration, $\overline{C_{bconc}}$ is the cuttings concentration for a stationary bed (not corrected by drilling fluid apparent viscosity) (%).

3.3 Methodology

A case study provided by Xiang (2016) was picked to validate the accuracy of Larsen's model in predicting the cuttings concentration. The detailed data of the flow loop and experiments was summarized in Table 3.2, Table 3.3 and Table 3.4. Table 3.4 data is calculated based on Table 3.3 with the shear rate between 100 and 200 RPM, as Rostami (2017) suggested that this shear rate ranges could provide a most favorable agreement with the annular measurements for HDD industry.

Table 3.2 flow loop and relative equipment parameters (Xiang, 2016)

Parameters	Value	Unit
Inner diameter of borehole	6	inch
Outer diameter of drill pipe	3.5	inch
Eccentricity	0.75	-
Cuttings size	1	mm
Rate of penetration (ROP)	10	m/h
Drilling fluid density	1050	kg/m^3

Table 3.3 Drilling fluid rheological properties (Xiang, 2016)

Drilling fluid No.	Viscometer reading (degree of Fann)					
	θ_{600}	θ_{300}	θ_{200}	θ_{100}	θ_{6}	θ_{3}
1	16.5	11	9.5	6	2	1.5
2	22	15	12	8	3	2
3	30	21	17	12	3.5	3
4	46	33	28	21	8	6

Table 3.4 Drilling fluid Bingham Plastic model parameter (Xiang, 2016)

Drilling fluid No.	Bingham Plastic model parameter	
	Yield stress (Pa)	Plastic viscosity (Pa*s)
1	6.63	0.0105
2	8.16	0.012
3	11.22	0.015
4	17.85	0.021

3.4 Result

3.4.1 Cuttings concentration for a stationary bed

Table 3.5, 3.6, 3.7, and 3.8 showed the calculated cuttings concentration and corresponding stationary bed height calculated by Larsen's model. Based on Cho et al. (2001) research, the mean volumetric concentration in a cuttings-bed with 95 % confidence interval is between 0.4503 and 0.5107, and the conclusion can be applied to any type of rock formation, regardless of rock types. Considering the tested cuttings were sand, the porosity of cuttings bed was chosen as 0.45 in the calculus.

Table 3.5. Drilling Fluid No.1: Stationary bed height calculated by Larsen's model and measured by Xiang (2016)

Drilling fluid No.1			
Flow velocity (m/s)	Calculated by Larsen's model		Experimental data measured by Xia (2016)
	Cuttings concentration for a stationary bed (%)	Corresponding stationary bed height (%)	Cuttings bed height (%)
0.8	20.81	19.5	29.4
0.9	17.52	17.3	24
1	14.22	15	19
1.1	10.94	12.5	14.3
1.2	7.64	9.8	9
1.3	4.35	6.7	3.8

Table 3.6. Drilling Fluid No.2: Stationary bed height calculated by Larsen's model and measured by Xiang (2016)

Drilling fluid No.2			
Flow velocity (m/s)	Calculated by Larsen's model		Experimental data measured by Xia (2016)
	Cuttings concentration for a stationary bed (%)	Corresponding stationary bed height (%)	Cuttings bed height (%)
0.8	21.04	19.6	23.5
0.9	17.92	17.5	20
1	14.79	15.4	16
1.1	11.67	13	12
1.2	8.54	10.4	8
1.3	5.42	7.7	3.2

Table 3.7 Drilling Fluid No.3: Stationary bed height calculated by Larsen's model and measured by Xiang (2016)

Drilling fluid No.3			
Flow velocity (m/s)	Calculated by Larsen's model		Experimental data measured by Xia (2016)
	Cuttings concentration for a stationary bed (%)	Corresponding stationary bed height (%)	Cuttings bed height (%)
0.8	21.95	20.2	20.7
0.9	19.19	18.4	18
1	16.43	16.6	14.5
1.1	13.67	14.6	11
1.2	10.91	12.5	7
1.3	8.14	10.2	3.2

Table 3.8 Drilling Fluid No.4: Stationary bed height calculated by Larsen's model and

measured by Xiang (2016)

Drilling fluid No.4			
Flow velocity (m/s)	Calculated by Larsen's model		Experimental data measured by Xia (2016)
	Cuttings concentration for a stationary bed (%)	Corresponding stationary bed height (%)	Cuttings bed height (%)
0.8	22.58	20.5	19
0.9	20.38	19.2	16.5
1	18.17	17.7	13.5
1.1	15.97	16.2	10
1.2	13.77	14.6	6.7
1.3	11.57	13	3.2

Figure 3.1, 3.2, 3.3, and 3.4 showed the comparisons between Larsen's model calculation and Xiang's experimental data in scatter diagram.

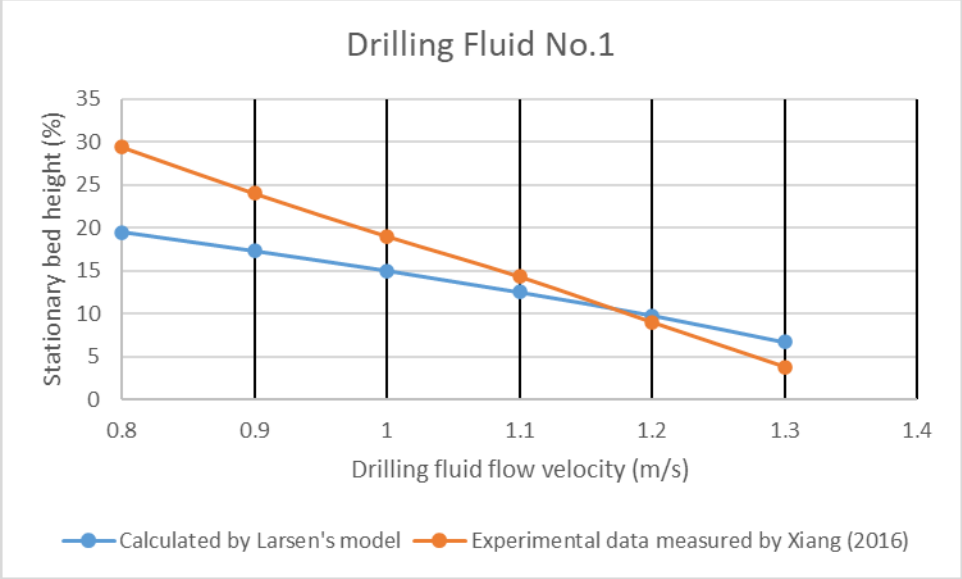

Figure 3.1, Drilling Fluid No.1: Stationary bed height calculated by Larsen's model and measured by Xiang (2016)

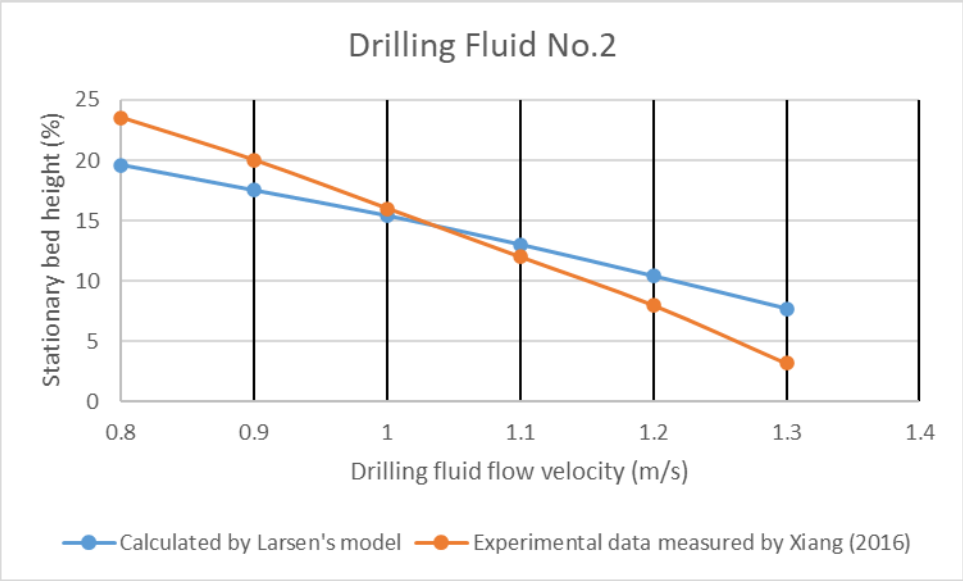

Figure 3.2, Drilling Fluid No.2: Stationary bed height calculated by Larsen's model and measured by Xiang (2016)

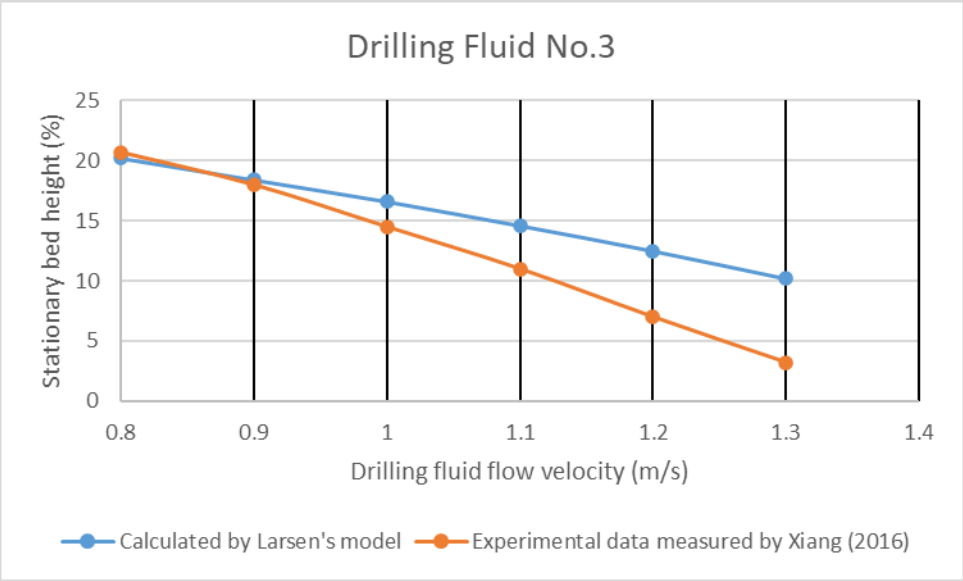

Figure 3.3 Drilling Fluid No.3: Stationary bed height calculated by Larsen's model and measured by Xiang (2016)

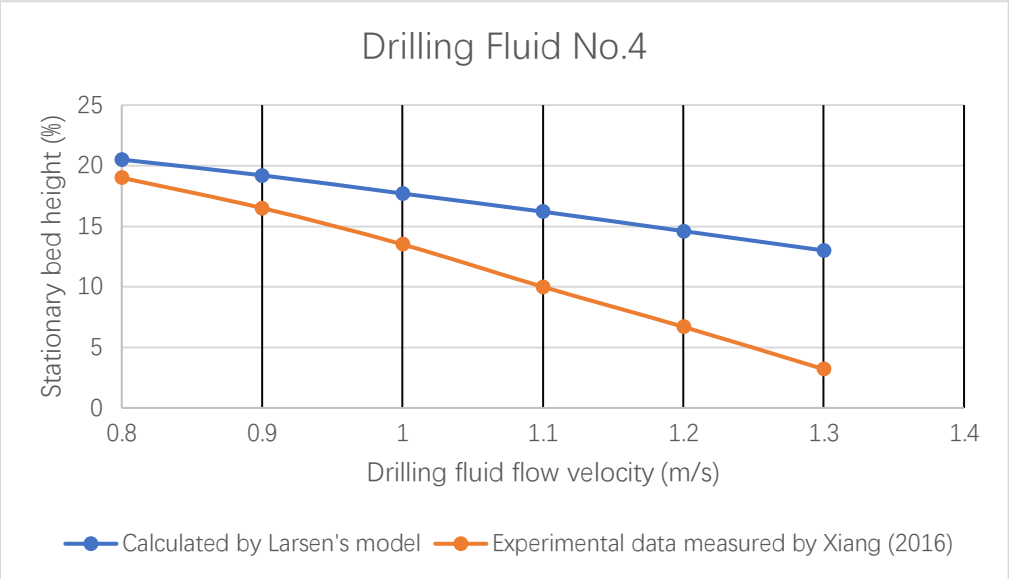

Figure 3.4 Drilling Fluid No.3: Stationary bed height calculated by Larsen's model and measured by Xiang (2016)

Compared with the experimental data measured by Xiang (2016), Larsen's model showed similar trend in predicting the decrease of stationary bed height with the increasing drilling fluid flow velocity for 4 different types of drilling fluid. For drilling fluid No.2, the estimated cuttings stationary bed height was almost the same as Xiang's experimental data when drilling fluid was circulated at 1m/s. For other types of drilling fluid, the fitness of Larsen's model compared with measured data is not ideal. On average, Larsen's model overestimates the cuttings bed height at high flow velocity and underestimates the cuttings bed at low flow rate.

It could be clearly seen that the slope of Larsen's model's scatter diagram was obviously smaller than that of Xiang's experimental data. To some extent, Larsen's model could not

reflect the rapid change of cuttings stationary height change caused by the variance of drilling fluid flow velocity. Based on the trends showing in these figures, the “real” critical transport fluid velocities (CTFVs) derived from Xiang’s experimental data would be smaller than that estimated by Larsen’s model. In other words, Larsen’s model slightly overestimated the critical transport fluid velocity (CTFV) and provide relatively conservative design for CTFV.

Figure 3.5 shows the estimated stationary bed height estimated by Larsen’s model in the same chart and Figure 3.6 shows the measured stationary bed height from Xiang’s.

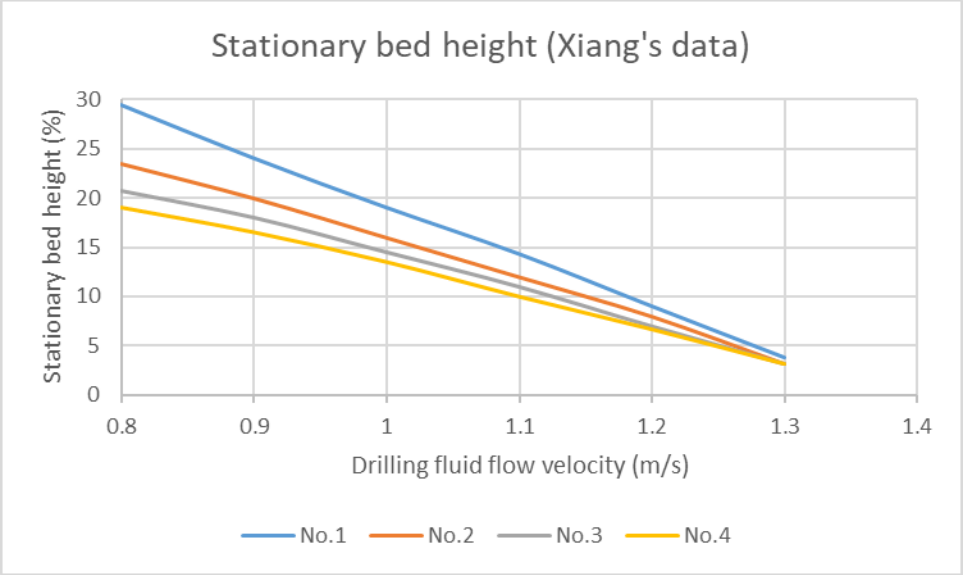

Figure 3.5: Measured stationary bed height (Xiang, 2016)

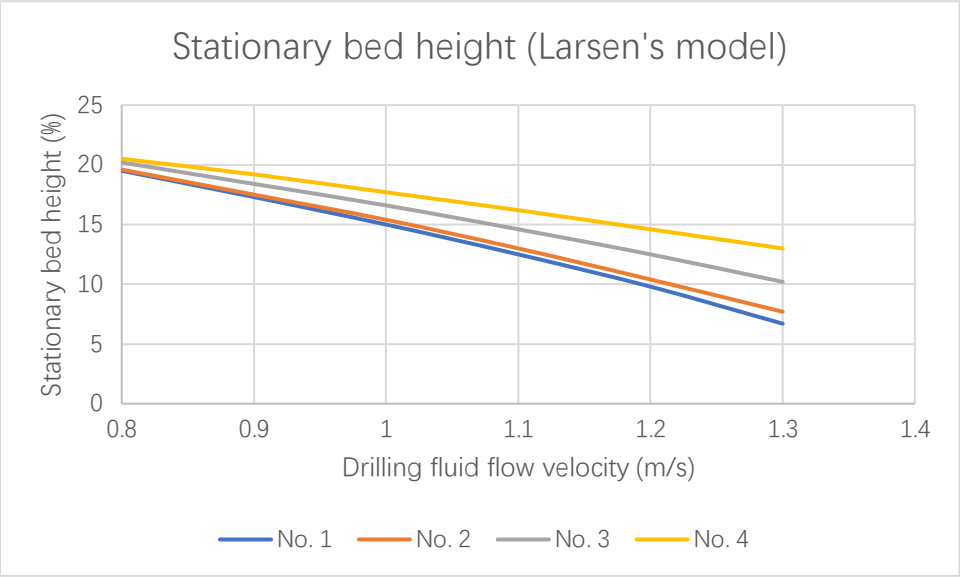

Figure 3.6: Estimated stationary bed height estimated by Larsen's model

From Figure 3.5, it could be found that the drill fluid rheological properties affect the dimensionless cuttings bed, but for high fluid velocity (1.1-1.3 m/s) the effect of drill fluid rheological properties become less apparent (Xiang, 2016), while Larsen's model doesn't reflect this behavior. Comparing these two figures, the hole cleaning performance of 4 types of different drilling fluid shows totally different trend. In Xiang's measurement, the No. 4 drilling fluid could have the best hole cleaning performance, while Larsen's model gives the opposite conclusion. To analyze the rheological parameters of the 4 types of drilling fluid in Table 3.6, another hole cleaning performance indicator YP/PV for drilling fluid is introduced. The higher the ratio of yield point to plastic viscosity (YP/PV), the better cuttings transport performed by drilling fluid (Deng, 2018; Okrajni and Azar, 1986). Table 3.9 summarizes the yield stress τ_y and YP/PV ratio of the drilling fluid used in Xiang's experiments.

Table 3.9: Yield stress and YP/PV ratio of drilling fluid

Drilling fluid No.	Yield stress (Pa)	YP/PV ratio
1	6.63	631.43
2	8.16	680
3	11.22	748
4	17.85	850

From the Table 3.9, it could be seen that drilling fluid No.4 have the highest YP/PV ratio. Combined with Deng's research (2018) - the suspension capacity of drilling fluid will be improved due to increasing of yield stress (τ_y), No. 4 drilling fluid will have the best cuttings transport performance. Xiang's results (2016) were consistent with the theory, while the results calculated from Larsen's model is not compliant with the theory.

3.4.2 Critical transport fluid velocity (CTFV)

Calculated by Larsen's model, the cuttings transport fluid velocity (CTFV) for 4 types of drilling fluid is summarized in Table 3.10. Suggested drilling fluid flow velocity calculated by HDD method was also included in Table 3.10. Based on the cuttings inject system in the flow loop, the porosity of soil was picked as 0. Due to the cuttings used in flow loop was sand, the Fluid-to-Soil ratio was considered as 3.

Table 3.10 Cuttings transport fluid velocity (CTFV) by Larsen's method and suggested flow velocity by HDD method

Drilling fluid No.	Critical transport flow velocity (m/s)	HDD method
1	1.43	0.0083
2	1.47	0.0083
3	1.59	0.0083
4	1.83	0.0083

HDD method only paid attention to the production of cuttings (ROP) for the drilling fluid flow velocity, which could not consider the effect of drilling fluid rheological properties, borehole inclination, etc. And the picked Fluid-to-Soil ratio was highly dependent on the engineering judgement. Larsen's model was also employed to estimate the possible cuttings concentration under drilling fluid flow velocity suggested by HDD model in this flow loop. The estimated cuttings concentration was 46.89%, which meant that cuttings bed would occupy nearly half space of the annulus.

3.5 Discussion

3.5.1 Larsen's model accuracy

Based on the comparisons between Xiang's experiment data and values calculated by Larsen's model based on experiment conditions, it could be concluded that Larsen's model provided roughly estimations for the cuttings bed height in small-scale borehole.

In some cases, Larsen's model could not consider the effect of drilling fluid rheological properties correctly. The error may be caused by the Bingham Plastic model used in Larsen's model. Larsen's model calculates the apparent viscosity of the non-Newtonian

drilling fluid based on BP model and uses it to estimate the equivalent slip velocity (ESV), while the BP model considers the viscoelastic property but ignores the shear-thinning property, which means that it could not completely perform the whole drilling fluid rheological properties.

Larsen's model estimates the cuttings transport fluid velocity (CTFV), indicating the minimum fluid velocity required to maintain a continuously upward movement of the cuttings (Larsen et al., 1997). In HDD pilot boring stage, CTFV with adequate coefficients may play a role of reference and guidance to evaluate the hole cleaning performance in the borehole.

Based on Rostami's research (2017), among three stage, pilot boring has the greatest construction concern due to the high risk of hydraulic fracture and loss of drilling fluid circulation. Overall, although Larsen's model has some defects including inadequate estimations of drilling fluid rheological properties and inaccurate estimations of cuttings bed height at low and high flow velocity, it could still be considered as a trial to indicate the hole cleaning performance in pilot boring stage of HDD project. What's more, there is still lack of suitable models to evaluate the hole cleaning performance in large-scale borehole, especially in the reaming process. Since the hole cleaning performance is directly related to a series of frequent problems in the HDD project and affects the project success, more precise models of drilling fluid minimum flow velocity for pilot boring stage and reaming stage are recommend in future research.

3.5.2 HDD method

To design the drilling fluid flow velocity, HDD method considers the cuttings production rate and cuttings characteristic but ignores a series of important influential factors including hole size and angle, drilling fluid rheological properties, etc. Based on HDD method, drilling fluid is circulated at a very low flow rate (approximately 1/20), compared with the critical transport flow velocity (CTFV) calculated by Larsen's model. Under the estimation of Larsen's model, the cuttings bed will occupy 46.89% space of the annulus. Considering that Larsen's model underestimates the cuttings bed height at low flow velocity, the cuttings bed space will be even larger. In this case, more researches are necessary to evaluate whether drilling fluid flow velocity calculated by HDD method could guaranteed sufficient hole cleaning performance.

3.6 Conclusion

The paper uses a case study to discuss the feasibility of Larsen's model to predict the cuttings stationary bed height and evaluate the hole cleaning performance in HDD pilot boring stage. Overall, Larsen's model could provide roughly estimations for cuttings stationary bed height in pilot boring stage (small-scale borehole), while overestimates the cuttings stationary bed height at high flow velocity and underestimates the cuttings stationary bed height at low flow velocity. In some cases, Larsen's model could not consider the effect of drilling fluid rheological properties correctly. Although Larsen's

model has some defects, it specifies a definite value - critical transport fluid velocity (CTFV), indicating when no cuttings would accumulate at the lower side of the wellbore. With suitable coefficients, the CTFV could be used as a reference for hole cleaning performance. The suggested drilling fluid flow velocity calculated by HDD method was far lower than the CTFV calculated by Larsen's model. In this case, the hole cleaning performance may be not ideal when drilling fluid is circulated at the velocity calculated by HDD method.

In the past three decades, HDD industry has experienced rapid development, and left some unsolved problems. To achieve sufficient hole cleaning performance, more appropriate models designed for HDD pilot boring stage and reaming stage are recommended in future research.

Chapter 4: Application of Delft Equation to estimate the maximum drilling fluid flow rate in HDD

4.1 Introduction

Trenchless technology is a new construction technology that uses all kinds of rock drilling equipment and technical means to lay, replace, or repair underground pipelines with little or no excavation (Wan et al., 2021). Among various trenchless technology, Horizontal Directional Drilling (HDD) is a trenchless technique that proposes several benefits over traditional open cut (Adel, Zayed, 2009). The method is the preferred installation option for telecommunication, electricity, and natural gas distribution facility owners due to its cost efficiencies and, among other benefits, its greatly reduced impact on the project site (Cohen and Ariaratnam, 2017). Today, HDD is a multi-billion dollar a year industry with hundreds of contractors and thousands of drilling rigs operating on five continents (Ariaratnam, 2009). In the construction of HDD, 3 stages are separated based on the drilling feature, which are pilot boring, reaming and pullback stages.

Since the application of HDD has been expanded from the installation of small utility pipelines and conduits to the installation of large diameter oil and gas transportation pipelines, plenty of research has been conducted to solve many technical problems encountered in practice (Shu and Ma, 2014). Gierczak (2014) concluded 38 risks in HDD technology, which were divided into 6 categories: mistakes in the HDD design, problems

with the HDD equipment, problems connected with the ground conditions, problems with supply, materials quality and the legal conditions in HDD, problems with the HDD construction works, environmental and safety problems and economic problems in HDD (Gierczak, 2014). In Gierczak's qualitative and quantitative analysis, the top five risks are downtime in the installation (18%), unexpected natural subsurface obstacles (15%), drilling fluid seepage (15%), unexpected man-made subsurface obstructions (11%), not taking into consideration the allowable bending radius of the drill pipes or the product pipe (10%). Among these risks, the drilling fluid seepage is considered as the one of the most frequent problems, which is directly related to the improper management of drilling fluid and borehole annular pressure, especially in the pilot boring stage.

Drilling fluid performs several different tasks including: (1) suspending and removing cuttings, (2) cleaning and lubricating the drill bit and pipe, (3) cooling electronic locating equipment, (4) increasing penetration rates, (5) minimizing hole erosion (i.e. stabilizing of the borehole), (6) creating buoyant force on the drill string and product pipe, (7) filling the annular space around product pipe (Ariaratnam et al., 2007). Drilling fluid management is a technique employed to maintain drilling fluid pressure between the maximum allowable and plan pressures during HDD, which prevents mud loss failure through the borehole and also provides the borehole with stability (Rostami, 2017).

There are still aspects of the practice that are not fully understood such as the uncontrolled fracturing of the soil surrounding the drilled conduit, which is also known as hydraulic

fracturing or “frac-out” (Kennedy et al., 2004). Hydraulic fracturing is a specific occurrence in non-fissured cohesive soils when the pressure of the drilling fluid exceeds the strength and confining stress of the surrounding soils, and the excess pressure fractures the soil around the bore (Farr, 2009). To quantify the maximum allowable pressure of the soils, Luger and Hergarden (1998) have developed a model based on the cavity expansion theory for assessment of the risk of inadvertent return (frac-out) in HDD (Park and Bayat, 2020). The current state-of-the-practice includes use of an equation developed at the Delft University of Technology, herein referred to as the Delft Equation (Delft Geotechnics, 1997; Kennedy et al., 2004).

Drilling fluid pressure in the borehole consists of two components, hydrostatic pressure and frictional pressure loss. Hydrostatic pressure is linked to drilling fluid density and cover depth, which are mainly controlled by drill path design. Frictional pressure loss is directly associated with two factors, drilling fluid rheological properties and drilling fluid flow rate. Drilling fluid rheological properties mainly refer to apparent viscosity and different parameters in different rheological models, such as plastic viscosity, yield point and consistency index.

Frictional pressure loss will increase with the increasing viscosity. Low frictional pressure loss caused by low viscosity will also reduce the risk of hydro fracture while allowing higher flow rate to be pumped to enhance cuttings bed erosion and cuttings transport distance (Deng, 2018). On the other hand, the high frictional pressure loss caused by

increasing flow velocity has been widely proved to be effective in improving cuttings bed erosion as well as enhancing the hole cleaning performance (Becker et al. 1991; Khatibi et al. 2018; Saasen 1998; Deng, 2018). As a result, increasing the frictional pressure loss by raising the drilling fluid flow rates within the borehole maximum allowable pressure is a practical choice to improve the hole cleaning performance.

In this study, maximum allowable pressures throughout the bore path were calculated to obtain the variation curve. Then, the drilling fluid hydrostatic pressure is calculated and discussed. With the hydrostatic pressure and maximum allowable pressure in the annulus, maximum frictional pressure loss could be calculated. As a result, the relative acceptable drilling fluid flow rates could be calculated and the variation curves of the maximum flow rates along the borehole were discussed.

4.2 Background

4.2.1 Maximum allowable pressure estimation

In order to allow the drilling mud to flow back and at the same time transport cuttings back to the ground surface, the drilling mud pressure in the borehole must be large enough to overcome the static mud pressure and the pressure loss during the circulation, while the drilling mud pressure should be limited to a certain value to prevent potential risk of hydro fracture (Shu and Ma, 2016; Shu et al., 2018). From another point of view, drilling fluid pressure in the annulus has an upper boundary, which is the maximum allowable pressure.

Multiple analytical and numerical methods were developed to evaluate the maximum allowable HDD drilling fluid pressure. Luger and Hergarden (1988) established a method using the cylindrical cavity expansion theory, which is the original Delft Equation. After that, different researchers (eg. Keulen, 2001; Kennedy et al, 2004; Xia, 2009; Staheli, 2010; Yan et al., 2016; Rostami, 2017; Lan and Moore, 2018; Lan and Moore, 2022) have continuously made contributions to improve or modify the original Delft equation (Shu et al., 2018). Details about their contributions and add-on are discussed in Chapter 2. With the Delft Equation, the maximum allowable drilling fluid pressure could be calculated as:

$$P_{max} = u + [\sigma_0' * (1 + sin\varphi) + c * cos\varphi + c * cot\varphi] * \left(\left(\frac{R_0}{R_{pmax}}\right)^2 + \frac{\sigma_0' * sin\varphi + c * cos\varphi}{G}\right)^{\frac{-sin\varphi}{1+sin\varphi}} - c * cot\varphi \qquad (4-1)$$

The symbols are defined below:

P_{max} refers to maximum allowable pressure in the annulus (Pa).

u refers to initial in-situ pore pressure (Pa).

φ refers to friction angle of soil (degree).

R_0 refers to borehole radius (m).

G refers to shear modulus (Pa).

c refers to cohesion coefficient (Pa).

R_{pmax} refers to the plastic zone (m). A factor of safety (FoS) may be applied (m).

σ_0' refers to effective stress (Pa) which is dependent on depth and soil conditions, defined by $\gamma * (h_{tot} - h_w) + \gamma' * h_w$

The key to successful use of the Delft Equation is to make proper judgement of the plastic zone R_{pmax}. Xia (2009) investigated that the Delft Equation overestimated the maximum allowable pressure when choosing plastic zone radius R_{pmax} as 2/3 overburden depth. Xia (2009) suggested a minimum Factor of Safety 2.5 should be applied when using Delft Equation to estimate the maximum allowable pressure. Staheli (2010) suggested that the accuracy of the predicted maximum pressure could be improved by picking small plastic zone radius R_{pmax} (2 – 3 borehole diameters or less). Staheli (2010) also concluded that shear modulus, height of soil, height of water and cohesion had the greatest effect on Delft Equation outcome. Similarly, Rostami (2017) investigated that the overburden depth, friction angle, and elastic modulus of soils had the highest impact on the limit pressure.

4.2.2 Annular pressure prediction

Drilling fluid annular pressure is comprised of 2 components, which are hydrostatic pressure and frictional pressure loss. The annular pressure could be expressed as:

$$P = P_s + P_f \tag{4-2}$$

Where the P_s is the hydrostatic pressure and P_f is the frictional pressure loss.

The hydrostatic pressure could be calculated with the following equation (Mitchell and Miska, 2011):

$$P_s = \rho * g * \Delta Z \tag{4-3}$$

The symbols are defined below:

P_s refers to hydrostatic pressure (Pa).

ρ refers to density of drilling fluid, including the produced cutting (kg/m^3).

g refers to the acceleration of gravity (N/kg).

ΔZ refers to elevation difference (m) between the drill rig entry point and the point of interest within the bore.

Frictional pressure loss is directly related to drilling fluid rheological properties, which means proper rheological models are needed to be employed in the calculation. Three rheological models, Newtonian, Bingham Plastic, and Power-law model are introduced in the chapter 2. Among these rheological models, Bingham Plastic model and Power-law model fits the drilling fluid properties well and widely used in HDD industry. This paper chooses Bingham Plastic model to quantify the drilling fluid rheological properties. The Bingham model requires an initial shear stress to initiate the fluid to flow, called the yield point (τ_y); at greater stresses, the fluid exhibits Newtonian behavior, where the plastic viscosity (μ_p) remains constant with increasing shear rate (Rostami, 2017). Its expression

is shown below:

$$\tau = \tau_y + \mu_p * \gamma \tag{4-4}$$

The symbols are defined below:

τ_y: Yield point (stress) (Pa), could be calculate from $\theta_{300} - \mu_p$

μ_p: Plastic viscosity (Pa*s), could be calculated from $\theta_{600} - \theta_{300}$

τ: Shear stress (Pa)

γ: Shear rate (/s)

θ_{600}, θ_{300}: Dial reading of rheometer at 300 and 600 RPM

With the yield point and plastic viscosity obtained from the Bingham Plastic model, the frictional pressure loss gradient for the laminar flow in the annulus can be calculated by Equation 4-5: (Mitchell and Miska ,2011)

$$\frac{dP_f}{dL} = \frac{48 * \mu_p * v}{(D_B - D_{DP})^2} + \frac{6 * \tau_y}{D_B - D_{DP}} \tag{4-5}$$

In the drill path with length L, the total frictional pressure loss can be calculated as:

$$P_f = \left(\frac{48 * \mu_p * v}{(D_B - D_{DP})^2} + \frac{6 * \tau_y}{D_B - D_{DP}}\right) * L \tag{4-6}$$

In the back calculation, the flow rate at certain frictional pressure loss gradient is expressed as:

$$Q = \frac{\pi}{192 * \mu_p} * \frac{dP_f}{dL} * ({D_B}^2 - {D_{DP}}^2) * (D_B - D_{DP})^2 - \frac{\pi}{32 * \mu_p} * \tau_y * ({D_B}^2 - {D_{DP}}^2) * (D_B - D_{DP}) \quad (4-7)$$

The symbols are showing below:

P_f: Annular frictional pressure loss (Pa).

D_B: Diameter of the borehole (m).

D_{DP}: Diameter of the drill pipe (m).

v: Average velocity (m/s)

L: Drill path length (m)

4.2.3 Maximum flow rate prediction

With the calculated maximum allowable pressure P_{max} from Delft Equation, the maximum frictional pressure loss could be expressed as:

$$P_f = P_{max} - P_s \quad (4\text{-}8)$$

On the other hand, as the frictional pressure loss could be calculated with

$$P_f = \left(\frac{48 * \mu_p * v}{(D_B - D_{DP})^2} + \frac{6 * \tau_y}{D_B - D_{DP}}\right) * L \quad (4-9)$$

the frictional pressure loss gradient could be expressed as:

$$\frac{dP_f}{dL} = \frac{P_f}{L} \qquad (4-10)$$

With the calculated maximum frictional pressure loss gradient, the maximum allowable flow rates could be calculated as:

$$Q = \frac{\pi}{192 * \mu_p} * \frac{dP_f}{dL} * ({D_B}^2 - {D_{DP}}^2) * (D_B - D_{DP})^2 - \frac{\pi}{32 * \mu_p} * \tau_y * ({D_B}^2 - {D_{DP}}^2) * (D_B - D_{DP}) \qquad (4-11)$$

The symbols are showing below:

P_f: Annular frictional pressure loss (Pa).

D_B: Diameter of the borehole (m).

D_{DP}: Diameter of the drill pipe (m).

v: Average velocity (m/s)

L: Drill path length (m)

4.3 Methodology

A case study is designed to analyze the maximum flow rate change throughout the drilling process. The borehole diameter is designed to be 6 inches and drill pipe diameter is 2.5 inches. The ground geometry and soil parameters are gathered from project done by Staheli et al. (2010) and presented in Figure 4.1 and Table 4.1.

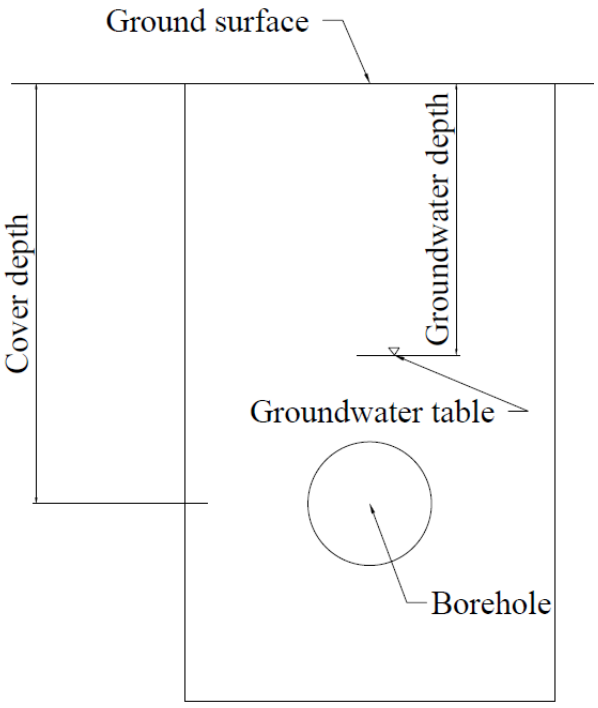

Figure 4.1. Ground geometry (Staheli et al., 2010)

Table 4.1. soil parameters (Staheli et al., 2010)

Soil parameters	SI unit	Imperial units
Groundwater depth	0 m	0 ft
Soil unit weright	20.42 kN/m^3	130 pcf
Internal friction angle	28°	28°
Cohesion	0	0
Shear modulus	4597 kPa	96000 psf

The drilling fluid chosen in the case study is 5% pure bentonite dispersion. where data is gathered from Su's thesis (2020). The summary of drilling fluid rheological properties is shown in Table 4.2

Table 4.2: Summary of drilling fluid rheological properties (Su, 2020)

5% pure bentonite dispersion		
Bingham plastic model parameters	Value	Unit
YP	7.168	Pa
PV	0.01	Pa·sec
YP	14.97	lbf/100 ft^2
PV	10.106	cP

The borehole geometry is designed with entry tangent, entry radius, horizontal tangent exit radius and exit tangent, which is showed in Figure 4.2

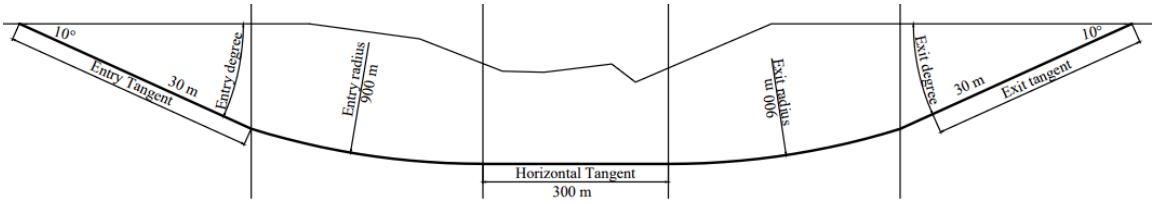

Figure 4.2. Drill path geometry

The designed value of each segment is summarized in the Table 4.3

Table 4.3. Drill path design

Parameters	Input data	SI Unit
Entrance degree	10	°
Exit degree	10	°
Entry Radius picked	900	m
Exit Radius picked	900	m
Entry Tangent	30	m
Exit Tangent	30	m
Horizontal Tangent	300	m

Overall, the drilling path details will be shown in Figure 4.3:

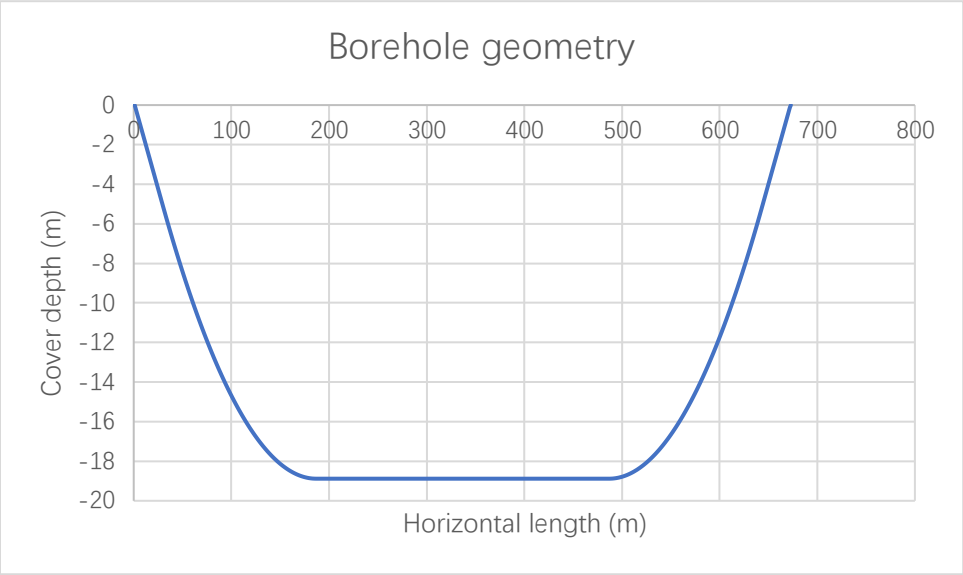

Figure 4.3 Borehole geometry

4.4 Result

4.4.1 Maximum allowable frictional pressure loss

Figure 4.4 shows the change of maximum allowable pressure, drilling fluid hydrostatic pressure and maximum frictional pressure loss throughout the drilling path.

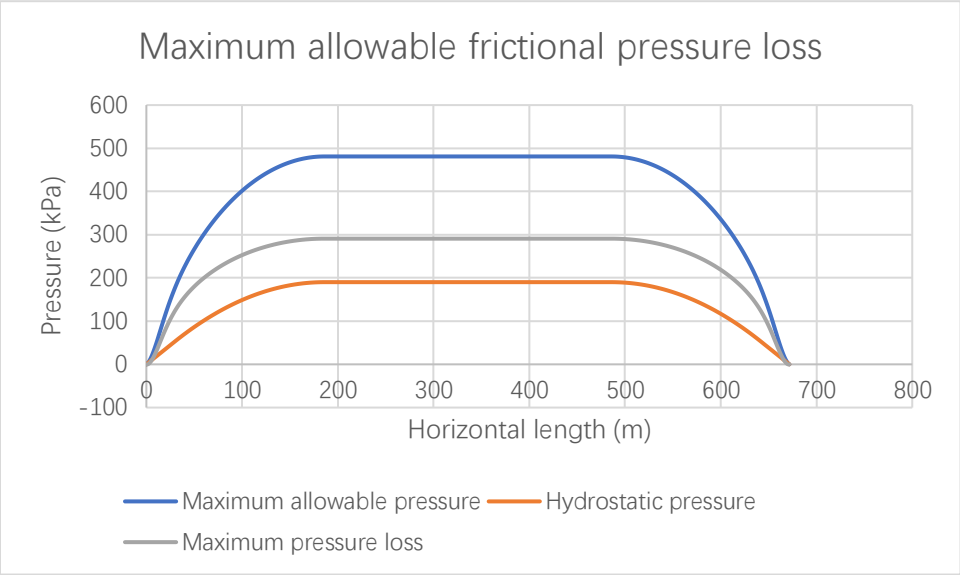

Figure 4.4 Change of maximum allowable pressure, drilling fluid hydrostatic pressure and maximum frictional pressure loss

The maximum allowable pressure and drilling fluid hydrostatic pressure change with the variance of the cover depth. As a result, maximum frictional pressure loss shows the same trend, which increases in entry tangent, entry radius; remains the same in horizontal tangent; decreases in exit radius and exit tangent.

4.4.2 Maximum flow velocity

On the other hand, with the borehole length increasing, maximum flow velocity in the annulus does not show similar trend. Figure 4.5 shows the maximum flow velocity trend and drill path in the same graph.

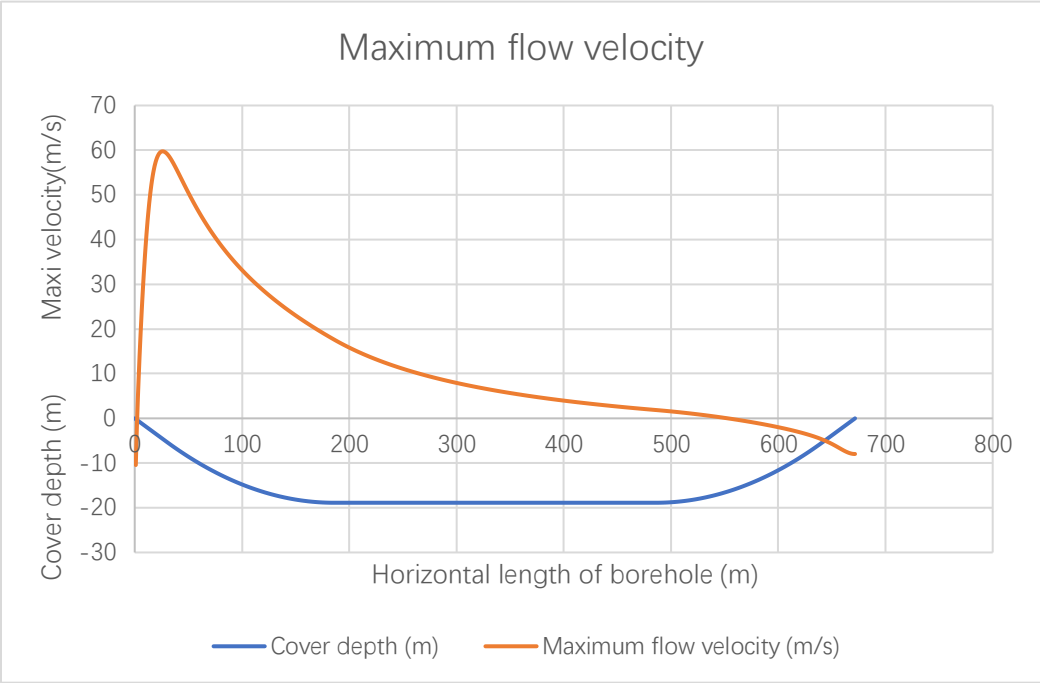

Figure 4.5 Maximum flow velocity profiles

From the profile, the maximum flow velocity could be even negative around the entry point and exit point, which means in these areas the total pressure will be higher the maximum allowable pressure calculated by Delft Equation even if the drilling fluid flow velocity equals to zero. In these sections of drill path, the borehole has a high risk of hydro fracture.

The maximum flow velocity increases at the beginning of the drilling process to a peak value (over 40 m/s) and decrease until the exit point. From the calculation of maximum flow rate, the deviations of the maximum flow velocity could be calculated.

$$v = \frac{4 * Q}{({D_B}^2 - {D_{DP}}^2) * \pi} \qquad (4-12)$$

$$Q = \frac{\pi}{192 * \mu_p} * \frac{dP_f}{dL} * ({D_B}^2 - {D_{DP}}^2) * (D_B - D_{DP})^2 - \frac{\pi}{32 * \mu_p} * \tau_y * ({D_B}^2 - {D_{DP}}^2) * (D_B - D_{DP}) \quad (4-13)$$

As

$$\frac{dP_f}{dL} = \frac{P_{f,max}}{L} \quad (4-14)$$

Therefore,

$$Q = \frac{\pi}{192 * \mu_p} * \frac{P_{f,max}}{L} * ({D_B}^2 - {D_{DP}}^2) * (D_B - D_{DP})^2 - \frac{\pi}{32 * \mu_p} * \tau_y * ({D_B}^2 - {D_{DP}}^2) * (D_B - D_{DP}) \quad (4-15)$$

Throughout the drilling process, the 2 variables are drill path length L and maximum frictional pressure loss $P_{f,max}$, while the drill pipe and borehole diameter, drilling fluid rheological properties remain the same and could be considered as constant. The total differential dQ of the Q could be calculated.

$$dQ = \left(\frac{\partial Q}{\partial L}\right) dL + \left(\frac{\partial Q}{\partial P_{f,max}}\right) dP_{f,max} \quad (4-16)$$

$$dQ = -\frac{1}{L^2} * P_{f,max} * \frac{\pi}{192 * \mu_p} * ({D_B}^2 - {D_{DP}}^2) * (D_B - D_{DP})^2 * dL + \frac{1}{L} * \frac{\pi}{192 * \mu_p} * ({D_B}^2 - {D_{DP}}^2) * (D_B - D_{DP})^2 * dP_{f,max} \quad (4-17)$$

$$\frac{dQ}{dL} = -\frac{1}{L^2} * P_{f,max} * \frac{\pi}{192 * \mu_p} * ({D_B}^2 - {D_{DP}}^2) * (D_B - D_{DP})^2 + \frac{1}{L} * \frac{\pi}{192 * \mu_p} * ({D_B}^2 - {D_{DP}}^2) * (D_B - D_{DP})^2 * \frac{dP_{f,max}}{dL} \quad (4-18)$$

At the peak point, $\frac{dQ}{dL}$ equals to zero.

$$\frac{dQ}{dL} = 0 \qquad (4-19)$$

$$-\frac{1}{L^2} * P_{f,max} * \frac{\pi}{192 * \mu_p} * ({D_B}^2 - {D_{DP}}^2) * (D_B - D_{DP})^2 + \frac{1}{L} * \frac{\pi}{192 * \mu_p} * ({D_B}^2 - {D_{DP}}^2) * (D_B - D_{DP})^2 * \frac{dP_{f,max}}{dL} = 0 \qquad (4-20)$$

$$\frac{dP_{f,max}}{dL} - \frac{P_{f,max}}{L} = 0 \qquad (4-21)$$

The peak point occurs when the increment of the maximum frictional pressure loss equals to the frictional pressure loss gradient. In this drill path, peak point will be located somewhere in entry tangent. After the peak point, the maximum flow velocity shows a down trend.

4.4.3 Maximum flow velocity distribution

Figure 4.6 shows the maximum flow velocity distribution along the drill path. Nearly 120 m parts of borehole near the exit point has a high risk of hydro fracture (calculated maximum flow velocities are less than 0).

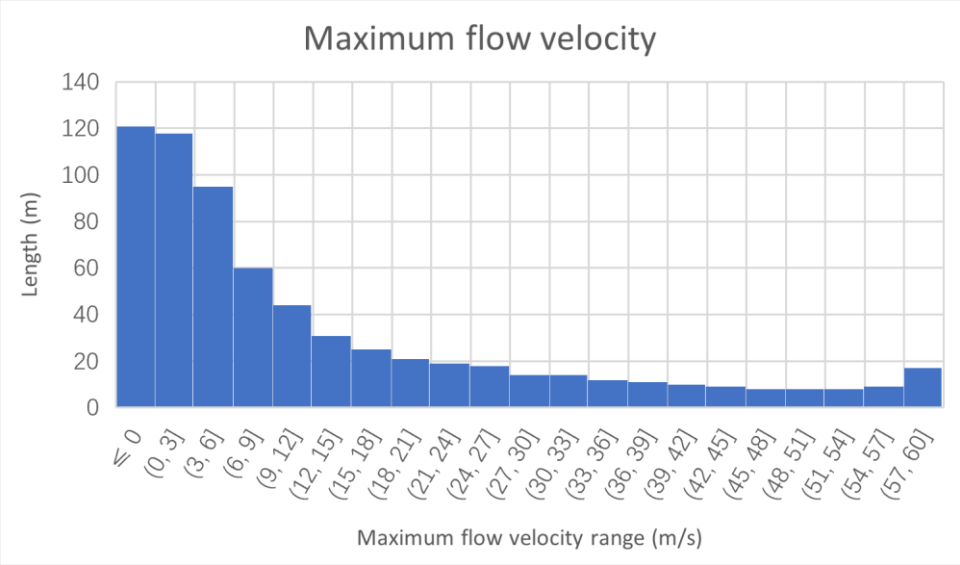

Figure 4.6 Maximum flow velocity distribution histogram

Figure 4.7 shows the maximum flow velocity distribution in percentage of total borehole length. Considering a drilling fluid circulating velocity 0.5 m/s, over 80% of the drill path is safe in pressure. What's more, over 55% of the drill path could allow the drilling fluid to be circulated at 5m/s. In this case, increasing the drilling fluid flow velocity in parts of the drill path during HDD pilot boring stage is practical and has great potential.

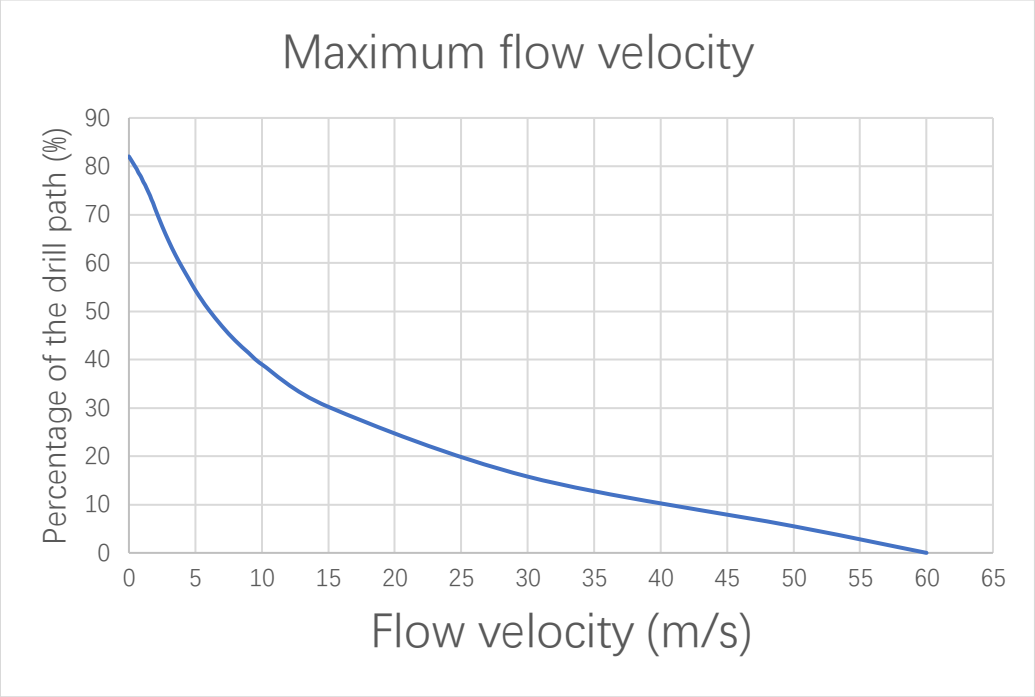

Figure 4.7 Maximum flow velocity distribution

4.5 Discussion

4.5.1 Risk of hydro fracturing

Based on maximum flow velocity calculus along the drill path showing on Figure 4.5, drill path near the entry point and exit point has a high risk of hydrofracturing. Reinforcement of borehole or other safety precautions are necessary for these parts in HDD pilot boring stage. However, Murray et al. (2014) researched the elevated annular pressure risk along the drill path and indicated that the majority (85%) of the elevated annular pressure risk events occur beyond the entry radius of the drill path, which is not correspond to the theorical analysis in this paper. Murray et al. concluded that the increasing of pressure

generally resulted from a restriction in the annular space caused by a buildup of cuttings.

4.4.2 Segmented flow velocity design

To solve the cuttings accumulation problems, increasing the drilling fluid flow rates is a sufficient solution. Figure 4.5 shows that the maximum flow velocity is highly enough in the entry radius and parts of horizontal tangent, which means that the circulated flow velocity has large potential for improvement. Instead of circulating the drilling fluid at the same velocity throughout the drilling process, a segmented drilling fluid flow velocity design may be better in cuttings transportation performance. Table 4.4 and Figure 4.8 shows the segmented flow velocity design.

Table 4.4 Segmented flow velocity design

Segmented flow velocity design		
Horizontal length		Designed flow velocity
Range (m)	Range (%)	m/s
0-2	0-0.30	1
2-265	0.30-39.45	5
265-341	39.45-50.77	3
341-399	50.77-59.41	2
399-671.66	59.41-100	1

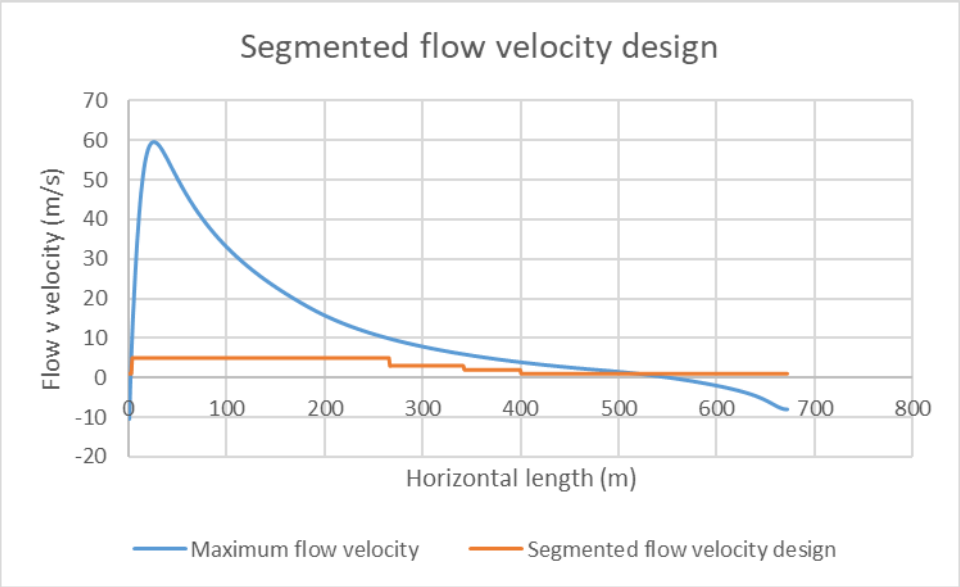

Figure 4.8 Segmented flow velocity design

Due to the possible restriction of pump ability and Factor of Safety (FoS) 2, the flow velocity gradients are designed to be 1, 3 and 5 m/s for convenience.

4.6 Conclusion

The paper uses the theorical approach to calculate maximum drilling fluid flow velocity along the drill path under the pressure limitation. A case study was designed to illustrate the variation of maximum flow velocity. Based on pressure analyses, high risk of hydro fracturing occurs near the entry and exit point. Throughout the drill path, it was found that the maximum flow velocity increased to a peak point where the increment of the maximum frictional pressure loss equaled to the frictional pressure loss gradient and decreased in the remaining path. In most of the drill path (80%), drilling fluid could be circulated at 0.5 m/s

and over half of the drill path (55%) drilling fluid could be circulated at 5 m/s. Overall, borehole annular pressure does not restrict the drilling fluid flow velocity in some part of drill path and drilling fluid flow velocity has high potential to raise in HDD pilot boring stage.

Based on Murray et al. (2014) research, most elevated annular pressure happens in the connections point of entry radius and horizontal tangent, but not the entry point and exit. Murray et al. (2014) concluded that the reason was the restriction in the annular space caused by a buildup of cuttings. To solve these problems, a segmented drilling fluid flow velocity plan may be designed and used in HDD industry to have a better hole cleaning performance.

Chapter 5: Conclusion and future research

5.1 Conclusion

In this thesis, a review on limitations for the drilling fluid flow rate was presented. 5 different empirical and theorical approaches to estimate the minimum flow velocity of drilling fluid were compared. Larsen's model was picked with a case study to analyze the minimum flow rate in the annulus. Another case study was conducted to evaluate the maximum flow rate throughout the drill path based on Delft Equation. The most important conclusions are highlighted below:

(1) In HDD industry, drilling fluid flow rate is restricted by maximum allowable pressure and cuttings transport performance in the annulus. Maximum allowable pressure limits the frictional pressure loss and further confines the maximum drilling fluid flow rates. On the other hand, sufficient hole cleaning performances necessitate a minimum drilling fluid flow rate to carry cuttings to the ground.

(2) Different close form solutions were developed to estimate the maximum borehole pressure in the annulus. Delft Equation was considered as a widely accepted practice in HDD industry. Researchers conducted various experiments to make improvements on its accuracy. To have a conservative estimate with Delft Equation, the plastic zone should be picked to a small value, or an additional factor of safety should be applied to the maximum borehole pressure.

(3) Drilling fluid annular pressure in HDD is comprised of hydrostatic pressure and frictional pressure loss. Hydrostatic pressure is related to drilling fluid density and cover depth, and frictional pressure loss depends on drilling fluid rheological properties, flow rate and borehole length. Frictional pressure loss induced by drilling fluid flow limits the increase of the flow rate in the annulus.

(4) Different theorical or empirical cuttings-transport models were developed in oil and gas engineering to quantify the minimum drilling fluid flow rate in the annulus. Skalle's model, Boyun's model, Mitchell's model, Ozbayoglu's model and Larsen's model were discussed in detail. Of five different models, Larsen's model provided the best accuracy for the minimum flow velocity predictions.

(5) Larsen's model provided a rough estimation for critical transport fluid velocity (CTFV) where cuttings would stop accumulating at the lower side of the wellbore. Although Larsen's model had some defects, including overestimating the cuttings stationary bed height at high flow velocity and underestimating the cuttings stationary bed height at low flow velocity as well as considering the drilling fluid rheological properties improperly, it could be used as an indicator and reference for hole cleaning performance until a more precise model is developed for HDD industry.

(6) Compared with the suggested drilling fluid flow velocity used in HDD industry, CTFV calculated with Larsen's model gave a far higher value. When drilling fluid is circulated

at the velocity calculated by HDD method, the cuttings bed height will be high and hole cleaning performance will be unsatisfactory.

(7) The maximum flow velocity increased to a peak point in where the increment of the maximum frictional pressure loss equaled to the frictional pressure loss gradient and decreased in the remaining path. The annular pressure will easily exceed the maximum allowable pressure near the entry and exit point, indicating high risk of hydro fracturing. Adequate reinforcement and casing are necessary in the exit and entry point.

(8) Based on the case study, in most of the drill path (80%), drilling fluid could be circulated at 0.5 m/s and over half of the drill path (55%) drilling fluid could be circulated at 5 m/s, which means that the drilling fluid flow velocity has high potential to raise in HDD pilot boring stage. A segmented drilling fluid circulating plan will greatly improve the hole cleaning performance.

5.2 Future Research

As HDD has some unique features, including highly inclined and horizontal borehole, shallow cover depth and water-based drilling fluid, a more appropriate flow loop system designed for HDD industry needs to be built to simulate the drilling fluid flow conditions in the future research. The flow loop will be designed for relatively larger borehole diameter, and may consist of horizontal section, entry radius and entry tangent, collecting data including annular pressure, hole inclination, drilling fluid flow rate, pipe eccentricity, rate of penetration (ROP), etc. Dr. Bayat's and his group dedicates to design and build a suitable flow loop for HDD industry.

A more accurate model for cuttings bed height and minimum flow rate, which consider a series of factors such as the pipe diameter, ROP, drilling fluid rheological properties, inclination angles, cutting characteristic, also needs to be developed with the proper flow loop. Afterwards, the original method to determine the drilling fluid circulating rate in HDD industry could be improved.

Reference

Adari, R. B., Miska, S., Kuru, E., Bern, P., & Saasen, A. (2000, October). Selecting drilling fluid properties and flow rates for effective hole cleaning in high-angle and horizontal wells. In *SPE Annual Technical Conference and Exhibition*. OnePetro.

Adeboye, Y. B., & Oyekunle, L. O. (2016). Experimental study of hole cleaning performance of underbalanced drilling at downhole conditions. *Nigerian Journal of Technology*, *35*(2), 375-380.

Adel, M., & Zayed, T. (2009). Productivity analysis of horizontal directional drilling. In *Pipelines 2009: Infrastructure's Hidden Assets* (pp. 835-843).

Allahvirdizadeh, P., Kuru, E., & Parlaktuna, M. (2016). Experimental investigation of solids transport in horizontal concentric annuli using water and drag reducing polymer-based fluids. *Journal of Natural Gas Science and Engineering*, *35*, 1070-1078.

Allouche, E. N., Ariaratnam, S. T., & Lueke, J. S. (2000). Horizontal directional drilling: Profile of an emerging industry. *Journal of Construction Engineering and Management*, *126*(1), 68-76.

Andresen, J., Consultants, T., & Staheli, K. (2019). *Engineering Judgement in Maximum Bore Pressure Design,* (NASTT) NASTT's 2019 No-Dig Show.

Andrew Farr. (2009). HDD Design Issues: Hydrofractures. Trenchless Technology.

Apaleke, A. S., Al-Majed, A. A., & Hossain, M. E. (2012, February). Drilling fluid: state of the art and future trend. Paper SPE 149555. In *SPE North Africa Technical Conference and Exhibition. Cairo, Egypt* (pp. 20-22).

Arends, G. (2003). Need and Possibilities for a quality push within the technique of horizontal directional drilling (HDD) Proceedings of 2003 No-Dig Conference. *Las Vegas, Nevada, March*.

Ariaratnam, S. T., Lueke, J. S., & Allouche, E. N. (1999). Utilization of trenchless construction methods by Canadian municipalities. *Journal of construction engineering and management*, *125*(2), 76-86.

Ariaratnam, Samuel & Stauber, Richard & Bell, Jason & Harbin, Bruce & Canon, Frank. (2003). Predicting and Controlling Hydraulic Fracturing during Horizontal Directional Drilling. 1334-1345. 10.1061/40690(2003)145.

Ariaratnam, S. T., Lueke, J. S., & Anderson, E. (2004). Reducing risks in unfavorable ground conditions during horizontal directional drilling. *Practice periodical on structural design and construction*, *9*(3), 164-169.

Ariaratnam, S. T., Harbin, B. C., & Stauber, R. L. (2007). Modeling of annular fluid pressures in horizontal boring. *Tunnelling and Underground Space Technology*, *22*(5-

6), 610-619.

Ariaratnam, S. T. (2009). Quality Assurance/Quality Control Measures in Horizontal Directional Drilling. In *ICPTT 2009: Advances and Experiences with Pipelines and Trenchless Technology for Water, Sewer, Gas, and Oil Applications* (pp. 1024-1036).

Bagnold, R. A. (1956). The flow of cohesionless grains in fluids. *Philosophical Transactions of the Royal Society of London. Series A, Mathematical and Physical Sciences*, *249*(964), 235-297.

Balcay, A., & Baser, T. (2019, November). Impact of Shear Modulus on Maximum Allowable Pressures in HDD. In *Geotechnical Engineering in the XXI Century: Lessons learned and future challenges: Proceedings of the XVI Pan-American Conference on Soil Mechanics and Geotechnical Engineering (XVI PCSMGE), 17-20 November 2019, Cancun, Mexico* (p. 39). IOS Press.

Baroid. 1997. Fluids Handbook. Baroid Fluid Services, Chapter 9, Rheology and Hydraulics, Haliburton, Houston, TX.

Baumert, M. E., Allouche, E. N., & Moore, I. D. (2005). Drilling fluid considerations in design of engineered horizontal directional drilling installations. *International Journal of Geomechanics*, *5*(4), 339-349.

Beljan, I. J. (2002). *Assessment of the annular space in a horizontal directional drilling*

installation (pp. 0233-0233). National Library of Canada= Bibliothèque nationale du Canada, Ottawa.

Bello, K. O., Oyeneyin, M. B., & Oluyemi, G. F. (2011, October). Minimum transport velocity models for suspended particles in multiphase flow revisited. In *SPE Annual Technical Conference and Exhibition*. OnePetro.

Bello, K., & Oyeneyin, B. (2016). Experimental investigation of sand minimum transport velocity in multiphase fluid flow in pipes. *Nigerian journal of technology*, *35*(3), 531-536.

Bilgesu, H. I., Mishra, N., & Ameri, S. (2007, October). Understanding the effect of drilling parameters on hole cleaning in horizontal and deviated wellbores using computational fluid dynamics. In *Eastern Regional Meeting*. OnePetro.

Becker, T. E., Azar, J. J., & Okrajnl, S. S. (1991). Correlations of mud rheological properties with cuttings-transport performance in directional drilling. *SPE Drilling Engineering*, *6*(01), 16-24.

Bennett, D., & Wallin, K. (2008). Step by step evaluation of hydrofracture risks for horizontal directional drilling projects. In *Pipelines 2008: Pipeline Asset Management: Maximizing Performance of our Pipeline Infrastructure* (pp. 1-10).

Boiko, A. V., Kirilovskiy, S. V., Maslov, A. A., & Poplavskaya, T. V. (2015). Engineering

modeling of the laminar–turbulent transition: Achievements and problems. *Journal of Applied Mechanics and Technical Physics*, *56*(5), 761-776.

Bourgoyne, A. T., Millheim, K. K., Chenevert, M. E., & Young, F. S. (1986). *Applied drilling engineering* (Vol. 2, p. 514). Richardson: Society of Petroleum Engineers.

Busahmin, B., Saeid, N. H., Alusta, G., & Zahran, E. S. M. (2017). Review on hole cleaning for horizontal wells. *ARPN J. Eng. Appl. Sci*, *12*(16), 4697-4708.

Caenn, R., & Chillingar, G. V. (1996). Drilling fluids: State of the art. *journal of petroleum science and engineering*, *14*(3-4), 221-230.

Caenn, R., Darley, H. C., & Gray, G. R. (2011). *Composition and properties of drilling and completion fluids*. Gulf professional publishing.

Cho, H., Shah, S. N., & Osisanya, S. O. (2001, September). Effects of fluid flow in a porous cuttings-bed on cuttings transport efficiency and hydraulics. In *SPE annual technical conference and exhibition*. OnePetro.

Chemwotei, S. C. (2011). Geothermal drilling fluids. Report, 10, 149-177.

Cohen, A., & Ariaratnam, S. T. (2017). Developing a Successful Specification for Horizontal Directional Drilling. In *Pipelines 2017* (pp. 553-563).

Deng, S. (2018). Assessment of Drilling Fluid Hole Cleaning Capacity in Horizontal

Directional Drilling–A Parametric Study of the Effects of Drilling Fluid Additives.

Ford, J. T., Peden, J. M., Oyeneyin, M. B., Gao, E., & Zarrough, R. (1990, September). Experimental investigation of drilled cuttings transport in inclined boreholes. In *SPE annual technical conference and exhibition*. OnePetro.

Geotechnics, D. (1997). A Report by Department of Foundations and Underground Engineering Prepared for O'Donnell Associates of Sugarland, TX.".

Gerasimova, V. (2016). Underground engineering and trenchless technologies at the defense of environment. *Procedia engineering*, *165*, 1395-1401.

Gierczak, M. (2014). The qualitative risk assessment of MINI, MIDI and MAXI horizontal directional drilling projects. *Tunnelling and Underground Space Technology*, *44*, 148-156.

Govier, G. W., & Aziz, K. (1972). The Flow of Complex Mixtures in Pipes; RE Krieger Pub. Co.: New York, NY, USA.

Guo, B., & Liu, G. (2011). *Applied drilling circulation systems: hydraulics, calculations and models*. Gulf Professional Publishing.

Hussaini, S. M., & Azar, J. J. (1983). Experimental study of drilled cuttings transport using common drilling muds. *Society of Petroleum Engineers Journal*, *23*(01), 11-20.

Hossain, M. E., & Al-Majed, A. A. (2015). *Fundamentals of sustainable drilling engineering*. John Wiley & Sons.

Jalukar, L. S., Azar, J. J., Pilehvari, A. A., & Shirazi, S. A. (1996, July). Extensive Experimental Investigation of Hole Size Effect on Cuttings Transport in Directional Well Drilling. In *ASME Fluids Engineering Division Annual Summer Meeting, San Diego, California, July* (pp. 7-12).

Jung, Y. J., & Sinha, S. K. (2007). Evaluation of trenchless technology methods for municipal infrastructure system. *Journal of infrastructure systems*, *13*(2), 144-156.

Kelessidis, V. C., & Bandelis, G. E. (2004). Flow patterns and minimum suspension velocity for efficient cuttings transport in horizontal and deviated wells in coiled-tubing drilling. *SPE Drilling & Completion*, *19*(04), 213-227.

Kennedy, M. J., Skinner, G. D., & Moore, I. D. (2004). Elastic calculations of limiting mud pressures to control hydro-fracturing during HDD. *Proc., No-Dig 2004*.

Keulen, B. (2001). "Maximum allowable pressures during horizontal directional drillings focused on sand." Delft Univ. of Technology, Delft, The Netherlands.

Khatibi, M., Time, R. W., & Shaibu, R. (2018). Dynamical feature of particle dunes in Newtonian and shear-thinning flows: relevance to hole-cleaning in pipe and annulus. *International Journal of Multiphase Flow*, *99*, 284-293.

Khodja, M., Khodja-Saber, M., Canselier, J. P., Cohaut, N., & Bergaya, F. (2010). Drilling fluid technology: performances and environmental considerations. *Products and services; from R&D to final solutions*, 227-256.

Kjøsnes, I., Løklingholm, G., Saasen, A., Syrstad, S. O., Agle, A., & Solvang, K. A. (2003, October). Successful water based drilling fluid design for optimizing hole cleaning and hole stability. In *SPE/IADC Middle East Drilling Technology Conference and Exhibition*. OnePetro.

Lan, H., & Moore, I. D. (2018). Practical criteria for assessment of horizontal borehole instability in saturated clay. *Tunnelling and Underground Space Technology*, *75*, 21-35.

Lan, H., & Moore, I. D. (2022). New design equation for maximum allowable mud pressure in sand during horizontal Directional drilling. *Tunnelling and Underground Space Technology*, *126*, 104543.

Larsen, T. I., Pilehvari, A. A., & Azar, J. J. (1997). Development of a new cuttings-transport model for high-angle wellbores including horizontal wells. *SPE Drilling & Completion*, *12*(02), 129-135.

Latorre, C. A., Wakeley, L. D., & Conroy, P. J. (2002). Guidelines for installation of utilities beneath Corps of Engineers levees using horizontal directional drilling. *Engineer Research and Development Center Vicksburg Geotechnical and Structures Lab*.

Li, Y., Bjorndalen, N., & Kuru, E. O. (2004, June). Numerical modelling of cuttings transport in horizontal wells using conventional drilling fluids. In *Canadian International Petroleum Conference*. OnePetro.

Luckham, P. F., & Rossi, S. (1999). The colloidal and rheological properties of bentonite suspensions. *Advances in colloid and interface science*, *82*(1-3), 43-92.

Luger, H. J., & Hergarden, H. J. A. M. (1988). Directional drilling in soft soil: Influence of mud pressures. *Proc. No-Dig, Int. Soc. Trenchless Technology*, 155-161.

Luo, Y. (1988). *Non-Newtonian annular flow and cuttings transport through drilling annuli at various angles* (Doctoral dissertation, Heriot-Watt University).

Mahmoud, H., Hamza, A., Nasser, M. S., Hussein, I. A., Ahmed, R., & Karami, H. (2020). Hole cleaning and drilling fluid sweeps in horizontal and deviated wells: Comprehensive review. *Journal of petroleum science and engineering*, *186*, 106748.

Ma, B., & Najafi, M. (2008). Development and applications of trenchless technology in China. *Tunnelling and Underground Space Technology*, *23*(4), 476-480.

Menezes, R. R., Marques, L. N., Campos, L. A., Ferreira, H. S., Santana, L. N. L., & Neves, G. A. (2010). Use of statistical design to study the influence of CMC on the rheological properties of bentonite dispersions for water-based drilling fluids. *Applied Clay Science*, *49*(1-2), 13-20.

Mitchell B (1995). Advanced oilwell drilling engineering, 10th edn. Mitchell Engineering, San Francisco.

Mitchell RF (2006). Petroleum engineering handbook volume II—Drilling engineering. Society of Petroleum Engineers, Richardson, Texas.

Mohamed, A., Salehi, S., & Ahmed, R. (2021). Rheological properties of drilling fluids containing special additives for geothermal drilling applications. In *The 46th Workshop on Geothermal Reservoir Engineering, Stanford, California, USA*.

Mohammadsalehi, M., & Malekzadeh, N. (2011, September). Optimization of hole cleaning and cutting removal in vertical, deviated and horizontal wells. In *SPE Asia Pacific Oil and Gas Conference and Exhibition*. OnePetro.

Moteleb, M., & Salem, O. (2004). Use of trenchless technologies in infrastructure rehabilitation and development. In *Pipeline Engineering and Construction: What's on the Horizon?* (pp. 1-10).

Murray, C., & Orlando, F. (2014). *Elevated Annular Pressure Risk in Horizontal Directional Drilling North American Society for Trenchless Technology (NASTT) NASTT's 2014 No-Dig Show*.

Najafi, M., Gokhale, S., Calderón, D. R., & Ma, B. (2021). *Trenchless technology: Pipeline and utility design, construction, and renewal*. McGraw-Hill Education.

Okrajni, S. S., & Azar, J. J. (1986). The effects of mud rheology on annular hole cleaning in directional wells. *SPE Drilling Engineering*, *1*(04), 297-308.

Osbak, M., Akbarzadeh, H., Bayat, A., & Murray, C. (2012). Investigation of horizontal directional drilling construction risks. *No-Dig Show*, 1-7.

Ouaer, H., & Gareche, M. (2018). The rheological behaviour of a water-soluble polymer (HEC) used in drilling fluids. *Journal of the Brazilian Society of Mechanical Sciences and Engineering*, *40*(8), 1-8.

Ozbayoglu, M. E., Saasen, A., Sorgun, M., & Svanes, K. (2010). Critical fluid velocities for removing cuttings bed inside horizontal and deviated wells. *Petroleum Science and Technology*, *28*(6), 594-602.

Park, I., & Bayat, A. (2020). Simplified Application of the Delft Method to Estimate Maximum Allowable Annular Pressure in HDD. In *Pipelines 2020* (pp. 559-573). Reston, VA: American Society of Civil Engineers.

Patino-Ramirez, F., Layhee, C., & Arson, C. (2020). Horizontal directional drilling (HDD) alignment optimization using ant colony optimization. *Tunnelling and Underground Space Technology*, *103*, 103450.

Pedrosa, C., Saasen, A., & Ytrehus, J. D. (2021). Fundamentals and physical principles for drilled cuttings transport—Cuttings bed sedimentation and erosion. *Energies*, *14*(3),

545.

Pilehvari, A. A., Azar, J. J., & Shirazi, S. A. (1999). State-of-the-art cuttings transport in horizontal wellbores. *SPE drilling & completion*, *14*(03), 196-200.

Piroozian, A., Ismail, I., Yaacob, Z., Babakhani, P., & Ismail, A. S. I. (2012). Impact of drilling fluid viscosity, velocity and hole inclination on cuttings transport in horizontal and highly deviated wells. *Journal of Petroleum Exploration and Production Technology*, *2*(3), 149-156.

Ramadan, A., Saasen, A., & Skalle, P. (2004). Application of the minimum transport velocity model for drag-reducing polymers. *Journal of Petroleum Science and Engineering*, *44*(3-4), 303-316.

Rostami, A., Yi, Y., Osbak, M., & Bayat, A. (2015). Parametric study on the maximum allowable pressure of drilling fluid during HDD based on the cavity expansion theory. In *Proceeding of NO-DIG conference 2015, Denver CO United States*.

Rostami, A. (2017). *Estimation of Plan Pressure and Maximum Allowable Pressure of Drilling Fluid during* Pilot Bore in Horizontal Directional Drilling

Reed, T. D., & Pilehvari, A. A. (1993, March). A new model for laminar, transitional, and turbulent flow of drilling muds. In *SPE Production Operations Symposium*. OnePetro.

Saasen, A. (1998, October). Hole cleaning during deviated drilling-The effects of pump

rate and rheology. In *European Petroleum Conference*. OnePetro.

Saasen, A., & Løklingholm, G. (2002, February). The effect of drilling fluid rheological properties on hole cleaning. In *IADC/SPE Drilling Conference*. OnePetro.

Sarireh, M., Najafi, M., & Slavin, L. (2013). Usage and applications of horizontal directional drilling. In *ICPTT 2012: Better Pipeline Infrastructure for a Better Life* (pp. 1835-1847).

Schaiter, B., & Girmscheid, G. (2008). HDD-horizontal directional drilling, pressure related failures caused by pilot drilling operations. *Innovations in Structural Engineering and Construction*, *2*, 1113-1118.

Shadizadeh, S. R., & Zoveidavianpoor, M. (2012). An experimental modeling of cuttings transport for an Iranian directional and horizontal well drilling. *Petroleum science and technology*, *30*(8), 786-799.

Shu, B., & Ma, B. (2015). Study of ground collapse induced by large-diameter horizontal directional drilling in a sand layer using numerical modeling. *Canadian Geotechnical Journal*, *52*(10), 1562-1574.

Shu, B., Ma, B., & Lan, H. (2015). Cuttings transport mechanism in a large-diameter HDD borehole. *Journal of Pipeline Systems Engineering and Practice*, *6*(4), 04014017.

Shu, B., & Ma, B. (2016). The return of drilling fluid in large diameter horizontal

directional drilling boreholes. *Tunnelling and Underground Space Technology*, *52*, 1-11.

Shu, B., Zhang, S., & Liang, M. (2018). Estimation of the maximum allowable drilling mud pressure for a horizontal directional drilling borehole in fractured rock mass. *Tunnelling and Underground Space Technology*, *72*, 64-72.

Skalle, P. (2011). *Drilling fluid engineering*. Bookboon.

Staheli, K., Christopher, G. P., & Wetter, L. (2010). Effectiveness of hydrofracture prediction for HDD design. *North American Society for Trenchless Technology (NASTT), Chicago, IL*, 1-10.

Su, Yi (2020). Impact of Suspended Cuttings on Drilling Fluid Rheology and Hole Cleaning Capacity in Horizontal Directional Drilling

Suleiman, M., Stevens, L., Jahren, C., Ceylan, H., Conway, W., & Design, I. S. U. (2010). *Identification of practices, design, construction, and repair using trenchless technology* (No. IHRB Project TR-570). Iowa State University. Institute for Transportation.

Tervydis, P., & Jankuniene, R. (2017). Horizontal directional drilling pilot bore simulation. *Turkish Journal of Electrical Engineering and Computer Sciences*, *25*(4), 3421-3434.

Tomren, P. H., & Azar, J. J. (1986). Experimental study of cuttings transport in directional wells. *SPE Drilling Engineering*, *1*(01), 43-56.

Thomas, D. G. (1962). Transport characteristics of suspensions: Part VI. Minimum transport velocity for large particle size suspensions in round horizontal pipes. *AIChE Journal*, *8*(3), 373-378.

Thomson, J., & Rumsey, P. (1997). Trenchless technology applications for utility installation. *Arboricultural Journal*, *21*(2), 137-143.

Umesh Dayal, N. J. W., & Rizzo, P. C. Trenchless Technology-An Overview.

Vroom, P., Profile, V., & Name:, Y. (2018). How to Plan and Mix Your Best HDD Drilling Fluid. Trenchless Technology

Vivas, C., Salehi, S., Tuttle, J. D., & Rickard, B. (2020). Challenges and opportunities of geothermal drilling for renewable energy generation. *GRC Transactions*, *44*, 904-918.

Wan, J., Jiang, S., Xia, Y., Li, J., & Li, G. (2021). Numerical model and program development of horizontal directional drilling for non-excavation technology. *Environmental Earth Sciences*, *80*(17), 1-21.

Westerweel, J., Boersma, B. J., & Nieuwstadt, F. T. (2016). *Turbulence: Introduction to Theory and Applications of Turbulent Flows*. Springer International Publishing.

Xia, H. (2009). *Investigation of maximum mud pressure within sand and clay during horizontal directional drilling* (Vol. 70, No. 02).

Xiang, H. (2016). LS-SVM Approach to Predict Cuttings Bed Height for Horizontal Well Bores. *Int. J. Simul. Syst. Sci. Technol*, *17*.

Yan, X., Ariaratnam, S. T., Dong, S., & Zeng, C. (2018). Horizontal directional drilling: State-of-the-art review of theory and applications. *Tunnelling and Underground Space Technology*, *72*, 162-173.

Yu, H. S., & Houlsby, G. T. (1991). Finite cavity expansion in dilatant soils: loading analysis. *Géotechnique*, *41*(2), 173-183.

Yu, H. S. (2000). *Cavity expansion methods in geomechanics*. Springer Science & Business Media.

Zaneldin, E. K. (2007). Trenchless construction: an emerging technology in United Arab Emirates. *Tunnelling and underground space technology*, *22*(1), 96-105.

Zeng, C., Yan, X., Zeng, Z., & Yang, S. (2018). The formation and broken of cuttings bed during reaming process in horizontal directional drilling. *Tunnelling and Underground Space Technology*, *76*, 21-29.